AD-A051 618 AUBURN UNIV ALA F/G 8/7
A STUDY OF THE SHEAR STRENGTH OF NORMALLY CONSOLIDATED ECUADORI--ETC(U)
DEC 77 J A BALL

UNCLASSIFIED NL

1 OF 2
AD
A051618

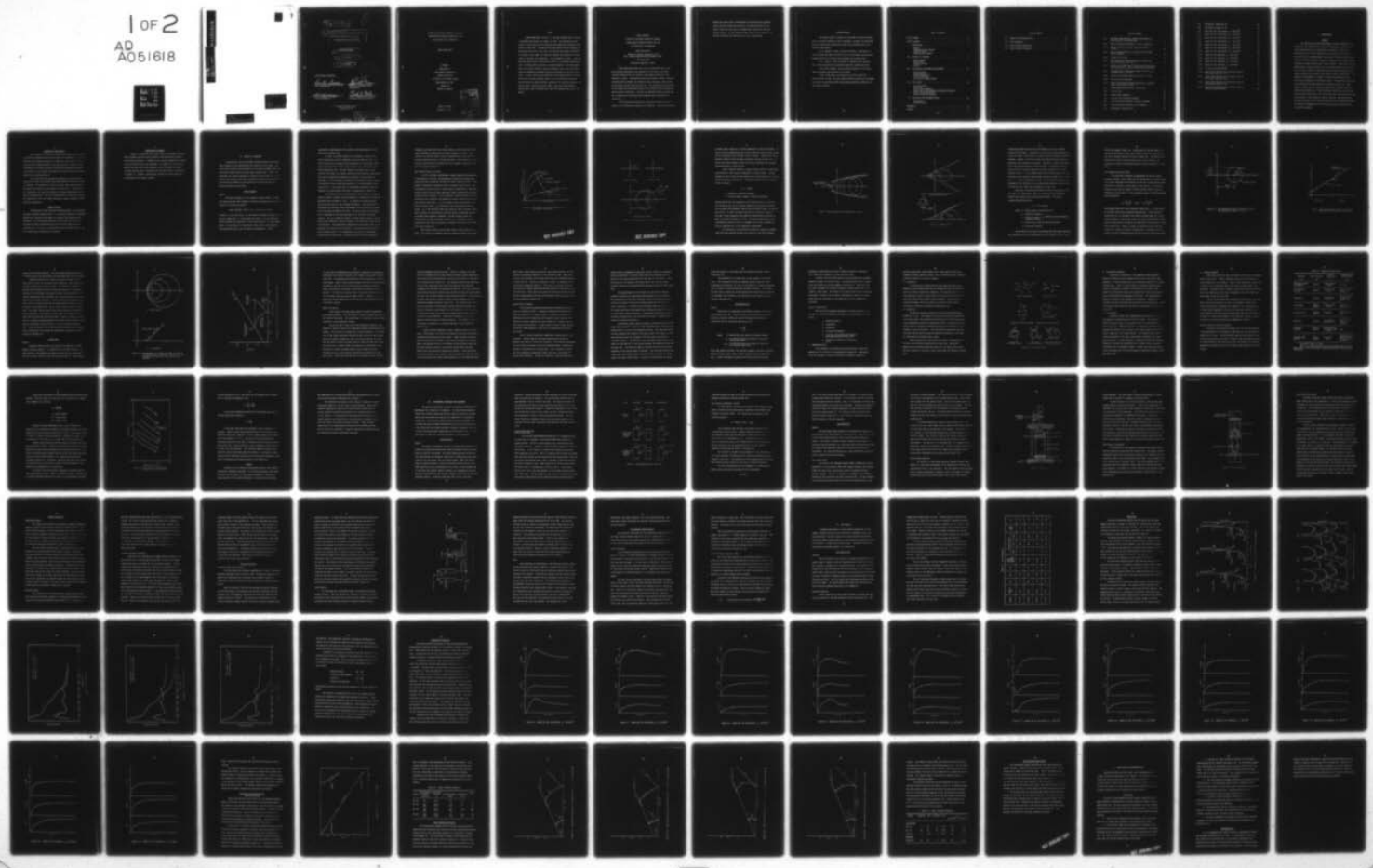

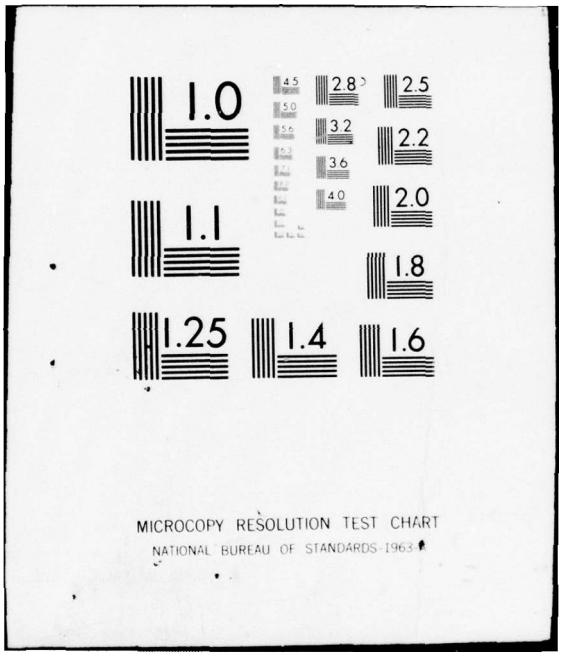
1.0
4.5
5.0
5.6
6.3
2.8
3.2
3.6
4.0
2.5
2.2
2.0
1.8
1.1
1.25
1.4
1.6
MICROCOPY RESOLUTION TEST CHART
NATIONAL BUREAU OF STANDARDS-1963-A

(9) Master's thesis,

(1)

(6) A STUDY OF THE SHEAR STRENGTH OF NORMALLY CONSOLIDATED ECUADORIAN VARVED CLAY AND ITS SENSITIVITY TO REMOLDING,

(10) James Andrew/Ball

(11) 8 Dec 77

(12) 100p.

Certificate of Approval:

R. K. Rainer
Rex K. Rainer, Professor and Head
Civil Engineering

Raymond K. Moore
Raymond K. Moore, Chairman
Assistant Professor, Civil
Engineering

Fred M. Hudson
Fred M. Hudson, Professor
Civil Engineering

Fred J. Molz
Fred J. Molz, Alumni Associate
Professor, Civil Engineering

Paul F. Parks, Dean
Graduate School

A STUDY OF THE SHEAR STRENGTH OF NORMALLY CONSOLIDATED ECUADORIAN VARVED CLAY AND ITS SENSITIVITY TO REMOLDING

James Andrew Ball

A Thesis

Submitted to

the Graduate Faculty of

Auburn University

in Partial Fulfillment of the

Requirements for the

Degree of

Master of Science

Auburn, Alabama

December 8, 1977

VITA

James Andrew Ball, son of J. A. and Lee (Falcone) Ball, was born in Red Bank, New Jersey, on October 13, 1947. He attended parochial schools in New Jersey and was graduated from Immaculate Conception High School in June 1965. He entered the United States Military Academy, at West Point, New York in July 1965, and received the degree of Bachelor of Science in June 1969. He received a Regular Army commission in the Corps of Engineers upon graduation. His assignments include: a tour in Maryland where he was a construction officer in an engineer battalion; a tour in Vietnam where he served as brigade engineer in the 3rd Brigade (Sep), 1st Cavalry Division, and base engineer; and a tour in Georgia where he commanded an Engineer Construction Company for one and a half years. In June, 1976, he was admitted to the Graduate School of Auburn University to pursue graduate study in Civil Engineering, attending Auburn University under the Army's advanced civil schooling program. He married Joan C. Arnold on June 8, 1969. They have three daughters: Suzanne Marie, age 7, Meredith Lee, age 4 and Courtney Anne, age 2 1/2 months.

THESIS ABSTRACT

A STUDY OF THE SHEAR STRENGTH OF NORMALLY CONSOLIDATED ECUADORIAN VARVED CLAY AND ITS SENSITIVITY TO REMOLDING

James Andrew Ball

Master of Science, December 8, 1977
(B.S., United States Military Academy, 1969)

100 Typed Pages

Directed by Raymond K. Moore

Consolidated-undrained (CU) triaxial compression tests, with pore pressure measurement, were employed in the study of the shear strength characteristics or normally consolidated varved clay from Guayaquil, Ecuador. Undisturbed samples were tested to obtain values of undrained shear strength, the effective stress envelope, stress-strain relationships and pore pressure build up. The mineralogical composition of the samples was determined through X-ray Diffraction and Thermogravimetric Analysis techniques. CU tests for remolded samples provided data for a comparison of undrained shear strengths and an evaluation of sensitivity.

Shear strength parameters were relatively consistent for all samples, with $\bar{\phi}$ decreasing slightly with remolding. Definite differences

between the stress-strain relationships of undisturbed and remolded samples existed; indicating a brittle, flocculated material in the natural state with high loss of strength upon remolding at the same moisture content. A_f and liquidity index values did not appear to be reliable indicators of sensitivity for this varved system.

ACKNOWLEDGEMENTS

The author wishes to express his gratitude and sincere appreciation to the Port Authority, Port of Guayaquil, Ecuador, for providing the soil samples that enabled this study to be conducted and to the following individuals:

To Dr. Raymond K. Moore, Assistant Professor, Department of Civil Engineering, Auburn University for his continuous assistance and guidance during this research and throughout my graduate study.

To Dr. James E. Laier, president of Southern Earth Sciences, Inc., whose cooperation and confidence made this research possible.

To Mr. Scott Koeppel, fellow graduate student, for his assistance throughout the completion of this work.

To Mrs. Sandy Ramey, for preparing the final manuscript.
And especially to Joan, his wife, whose unselfish support and invaluable assistance in typing the drafts helped make expeditious completion of this thesis possible.

TABLE OF CONTENTS

LIST OF TABLES

LIST OF FIGURES

I. INTRODUCTION

General

The laboratory and field measurement of shear strength of subsurface soil has remained one of the most challenging tasks and professional responsibilities of geotechnical engineering. Geotechnical knowledge will be of vital importance to the expansion of industrial facilities in the "underdeveloped" countries as the prices they receive for their diminishing natural resources increase and the revenues become available to support massive public works projects. During the next two decades many of these countries will be investing heavily in port facilities, and the locations of these facilities are often characterized by complex geotechnical conditions that require careful investigation. For example, the government of Ecuador is presently expanding the port facilities at Guayaquil on the Pacific Ocean. The subsurface conditions are characterized by deep deposits of saturated varved clay. These deposits present several significant geotechnical problems since the construction sequence will involve dredging, backfilling, and erection of heavy harbor facilities. The varved soils must therefore be assessed with respect to slope stability, bearing capacity, and consolidation. The shear strength of this particular material is of immense importance in the proper assessment of its performance during all phases of the construction sequence.

Statement of the Problem

Past studies of varved clay systems have focused on the soils of the northern hemisphere, particularly Canada and Scandinavia. The shear strength and deformation behavior of these soils has been observed, and various shear strength parameters have been measured. However, little information is currently available concerning the behavior of sedimentary deposits in the southern hemisphere that display similar structural properties and characteristics.

It is known that the engineering properties of an undisturbed varved soil system are different from those obtained if that soil system is remolded. The remolded soil usually displays lower shear strength parameters and different consolidation characteristics. The mineralogical composition, soil particle integrity, and phase relationships also play an important part in the full understanding of varved soil behavior. The complexity of this soil system represents a major challenge for geotechnical engineering.

Scope of Thesis

The objective of the study being reported herein is to determine the shear strength characteristics of a varved soil obtained in Guayaquil, Ecuador and to determine the amount of strength loss associated with remolding. The consolidated-undrained triaxial test was utilized to evaluate the shear strength characteristics of both undisturbed and remolded soils. To assist in understanding shear strength behavior, the soil mineralogical composition is estimated.

Organization of Report

Chapter II summarizes the current state of knowledge concerning shear strength, and the various graphical techniques used to analyze stress-state conditions. A summary of the current information on varved clays and sensitivity is also presented. In Chapter III, the triaxial testing and data acquisition equipment and the laboratory procedures utilized are described. A discussion of the test results is presented in Chapter IV. Chapter V contains the conclusions of this study and recommendations for further research.

II. REVIEW OF LITERATURE

Three specific and interrelated literature topics are particularly relevant to the understanding and analysis of this study. The first section reviews the development of soil shear strength theory and the current methods used to analyze shear strength data. Section two summarizes the current knowledge of varved clay and varved clay systems. Section three provides pertinent information concerning sensitive clays with particular emphasis on the mechanisms of sensitivity and soil physical property relationships.

Shear Strength

General

The shear strength of a soil depends on many factors. A function describing the shear strength or shearing resistance of a soil may contain the following variables:

$$\text{Shear strength} = F(e, \phi, C, \sigma', c', H, T, \varepsilon, \dot{\varepsilon}, S)$$

in which e is the void ratio, ϕ is the angle of internal friction, C is the soil composition, σ' is the effective stress, c' is the effective stress parameter for cohesion, H is the stress history, T is the temperature, ε is the strain, $\dot{\varepsilon}$ is the strain rate, and S is the structure. These parameters may or may not function independently. A full

quantitative understanding of the possible interrelationships is not available at present (18).

In order to quantify certain soil parameters, namely stress-strain properties, specific laboratory tests have been devised. The three primary tests to measure these properties on a macroscopic level are 1) the Direct Shear test, 2) the Triaxial Test, and 3) the Unconfined Compression Test. The most common and versatile test is the triaxial test, which is a special version of the cylindrical compression test used to determine the mechanical properties of many materials. Although it is not necessary to determine the strength of many construction materials using a confining pressure, it is often essential when testing soils. The triaxial test is considered a destructive test as compared to a consolidation test which is conducted as a model test.

The altering of the soil equilibrium stress state by a change in applied stresses, through a testing apparatus, is basically the means for determining the strength of a soil. As stresses are applied along a particular axis the soil will undergo deformation. The resistance to deformation by continuous shear displacement of soil particles is essentially the shear strength of the soil. The true nature of the deformation is dependent on the same parameters as in the shear resistance function. The soil eventually reaches a stress state at which it can no longer resist additional stress increases. This condition is the failure or yield point. The quantitative evaluation of the failure point may be dependent upon various failure criteria. For most materials and particularly cohesive soils, it is represented by the peak of the deviator stress-vertical strain curve. Certain soils will lose all structural

integrity, and their ability to resist stress, at the yield point while others continually deform with no further increase in stress. Soils exhibit a far greater range of failure characteristics than other construction materials such as concrete and steel. Typical deviator stress-vertical strain curves for various clay soils tested in undrained shear are illustrated in Figure 2.1.

Mohr-Coulomb Theory of Failure

In 1871, Otto Mohr contributed a rupture theory for the analysis of the behavior of solids; the mathematical formulation produced equations which have a graphical solution for stress state at a point. This graphical technique is popularly known as the Mohr stress circle. The representative stress circle is constructed by establishing a coordinate system in which the x-distance represents normal stresses and y-distance represents shear stresses. In soil mechanics, tensile stresses are comparatively rare; therefore, the compressive normal stresses are positive and plotted to the right. σ_1 is the largest stress and defined as the major principal stress. σ_2 is defined as the intermediate principal stress. σ_3 is the smallest stress and called the minor principal stress. Shear stresses are represented as absolute values of magnitude and may be plotted either upward or downward. The Mohr diagram allows the visualization of shear and normal stresses (σ, τ) acting on a plane, regardless of the plane's orientation, through a soil mass in two dimensions (25) (Figure 2.2).

Mohr failure theory also has been found to apply quite well to soils. The failure of a material does not depend on normal stress alone

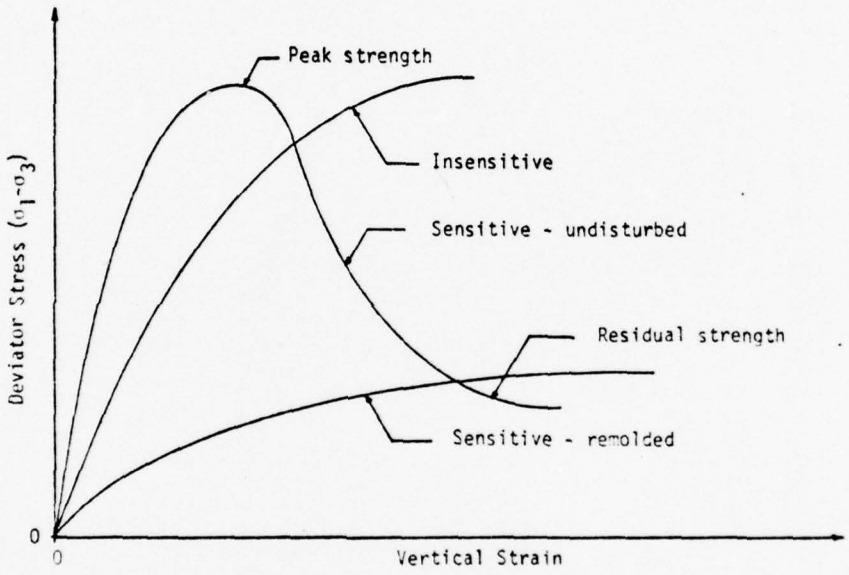

Figure 2.1. Deviator Stress - Vertical Strain Relationships for Clays Tested in Undrained Shear.

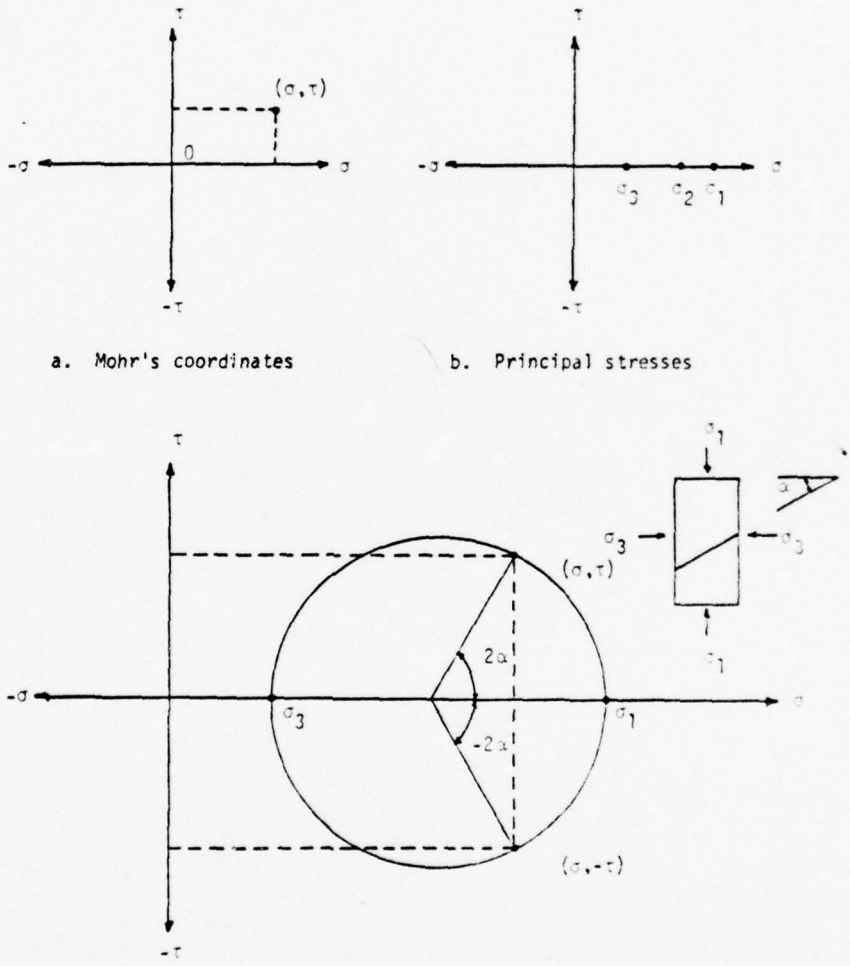

a. Mohr's coordinates

b. Principal stresses

c. Mohr's circle of stresses

Figure 2.2. Mohr's Coordinates and Mohr's Circle of Stresses.

or shear stress alone but a critical combination of the two stresses. A locus of points representing the critical value for various stress states can be constructed using the Mohr circle of stress. These points form a boundary commonly called the Mohr envelope of failure (Figure 2.3). A stress state that produces a Mohr circle which intercepts the strength envelope produces a shear failure.

Charles Augustin Coulomb, a famous French scientist, contributed significantly to the science of mechanics of elastic bodies. Coulomb assumed the laws of friction and cohesion for solid bodies were valid for granular materials such as soil. The yield criterion that he suggested (1773) is written

$$\tau \leq c + \sigma \tan \phi$$

c = cohesion or cohesion intercept

ϕ = friction angle or angle of shearing resistance

Coulomb stated that the magnitude of the shearing stress τ on any section through a mass of an isotropic cohesive soil must not be greater than an amount which depends linearly upon the normal stress σ acting on the section. In order to express the failure criterion in terms of principal stress components the graphical representation according to Mohr is used (23) (Figures 2.4, 2.5). It must be noted that σ_2, the intermediate principal stress, is assumed to be a minor influence on failure conditions and is not graphically represented.

The discovery of the principle of effective stress by Terzaghi (1923 and 1932) provided further clarification of the shear strength

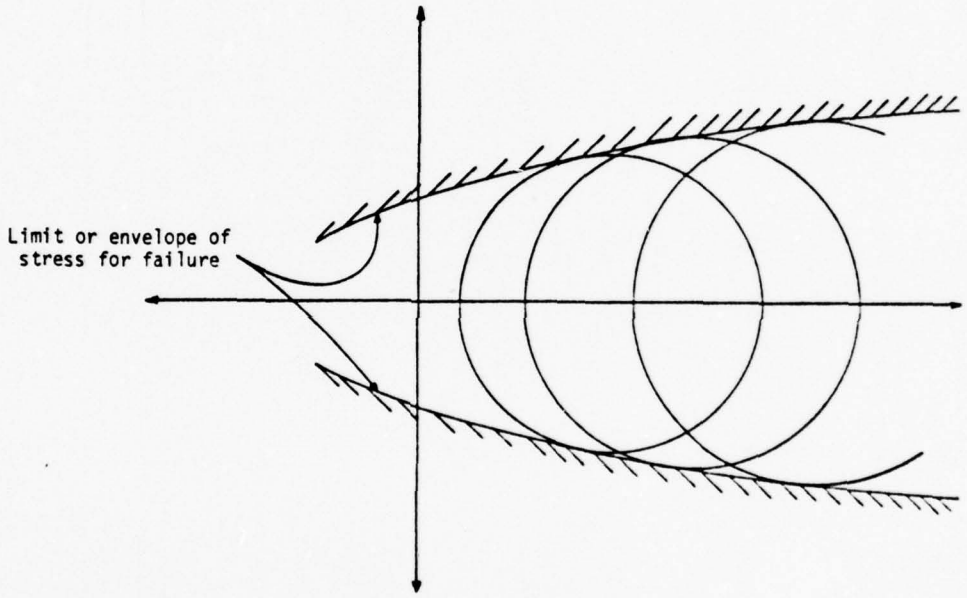

Figure 2.3. Mohr's Envelope of Failure Generated by Mohr's Circles.

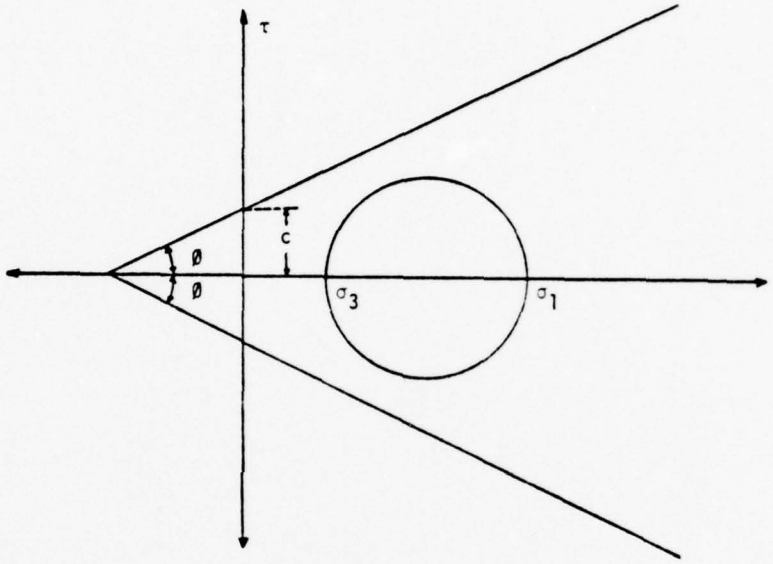

Figure 2.4. Mohr's Representation of a Stress and the Coulomb Yield Criterion.

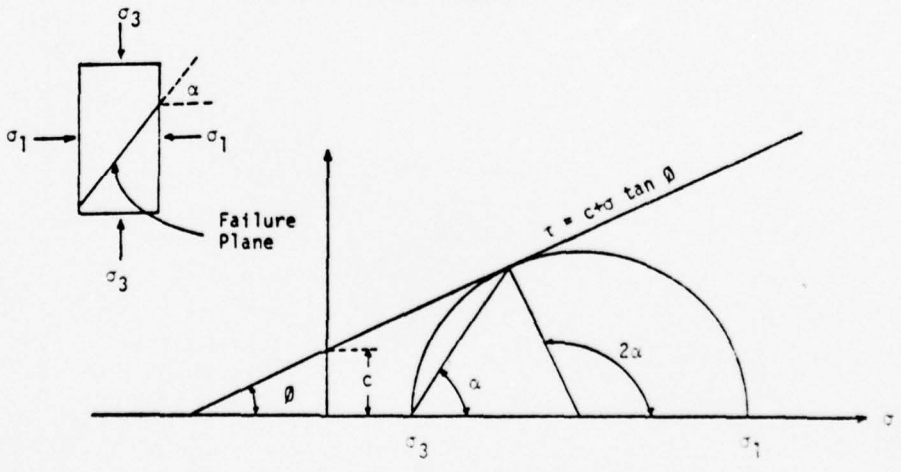

Figure 2.5. Stresses at Failure.

differences between sand and clay and enhanced the use of the Mohr-Coulomb failure theory. Previously, if the total principal stresses in a mass are known, the stresses at a point with any orientation could be computed. However, if the soil voids are filled with water the total principal stress consists of two parts. One part, u, acts in the water and is called pore pressure or neutral stress. The balance of stress acts strictly in the solid phase and is often referred to as "intergranular stress." In its simplest terms the principle asserts that the effective stress controls volume change and shear strength and is given by $\sigma' = \sigma - u$ for a saturated soil (18). By far the most important consequence of this discovery is an increased understanding of the behavior of cohesive soils since their permeability is very low.

Therefore, the maximum resistance to shear on any plane in the soil mass, on a macroscopic scale, is a function of the difference between total normal stress and the pore pressure. This may be expressed quantitatively as:

$$\tau = c' + (\sigma - u) \tan \phi'$$

where τ_f = shear stress on the failure plane

c' = effective cohesion

ϕ' = effective angle of internal friction

} effective stress parameters

σ = normal total stress on the failure plane

u = pore water pressure

The validity of the above relationships has been amply confirmed for saturated soils by the experimental work of Rendulic (1937), Taylor

(1944) and Laughton (1955) (2). Further work by Yong and McKeyes on the yield and failure of clay under triaxial stress has substantiated the use of the Mohr-Coulomb frictional rupture (33). The Mohr-Coulomb failure law is one of the most widely used in soil mechanics and accepted as a highly valid approximation of failure conditions in soils (14).

p-q Diagrams and Stress Paths

In large scale laboratory investigations of the soil shear strength, numerous stress states must be represented on a single diagram. It is quite cumbersome and confusing to plot Mohr circles and even more difficult to interpret a large number of test results. An alternate scheme has been devised (Lambe) in which the Mohr state of stress is plotted as a stress point. A new coordinate system is established where the relationships

$$p = \frac{\sigma_1 + \sigma_3}{2} \quad \text{and} \quad q = \frac{\sigma_1 - \sigma_3}{2}$$

are plotted along the x and y distances respectively. p is the center of the Mohr circle and q represents maximum shear. Each respective stress point (p, q) represents the state of maximum shear for a given stress condition. Knowing the values of p and q the entire Mohr circle may be reconstructed to determine the magnitude of the principal stresses (14) (Figure 2.6). Figure 2.7 shows an alternative way to plot the results of a series of triaxial strength tests. The points give the values of p and q corresponding to the peak points of the stress-strain

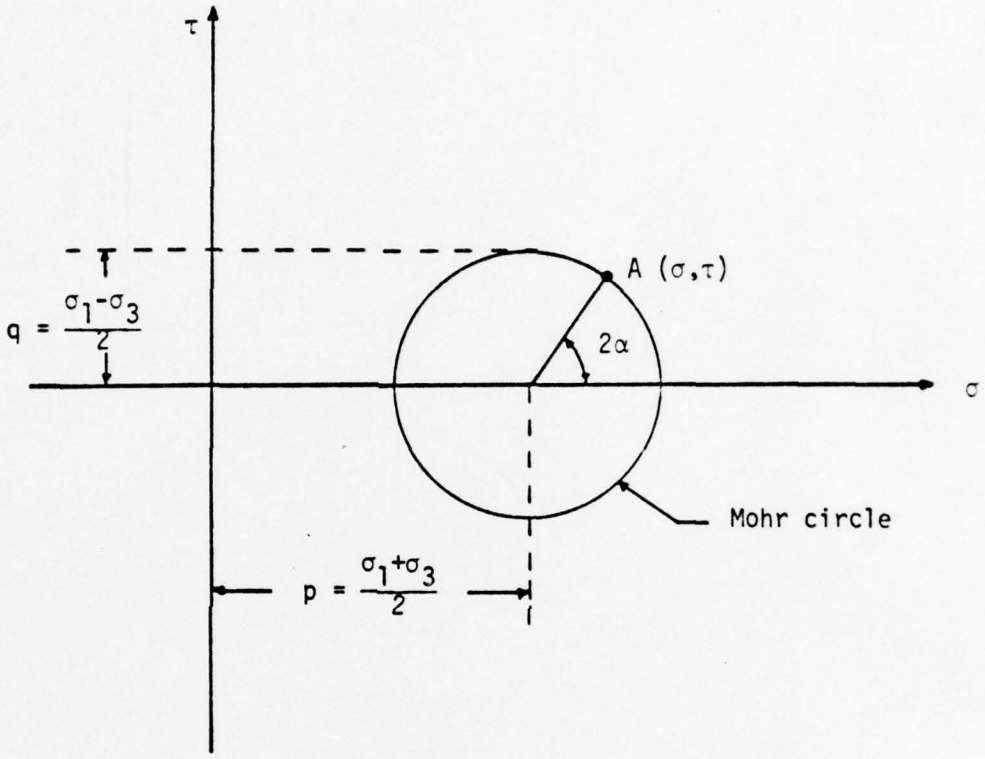

Figure 2.6. Mohr Diagram for State of Stress at a Point with Equivalent Values of p and q.

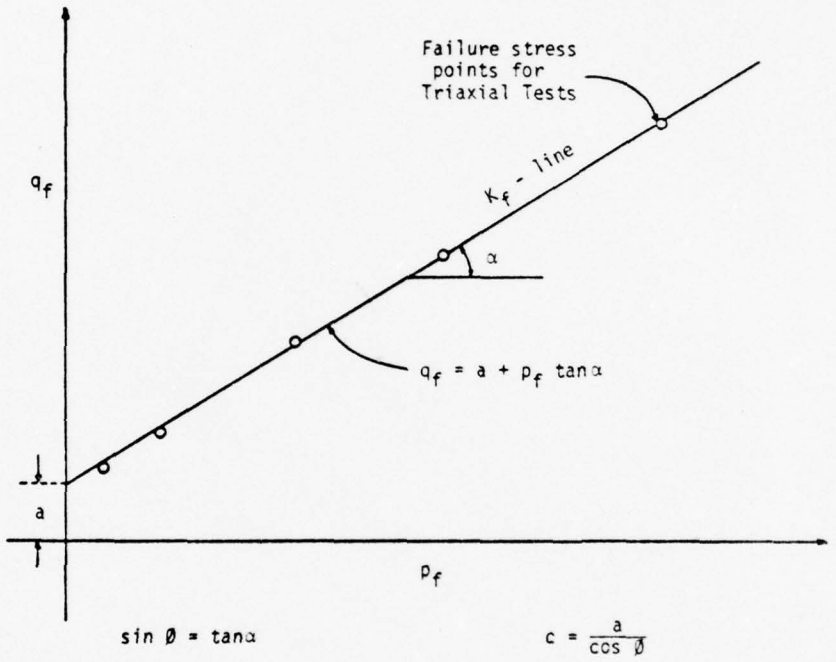

Figure 2.7. Results of Strength Test Plotted on p-q Diagram with Relationships of q_f and p_f to Mohr-Coulomb Envelope.

curves or the failure condition. The curve drawn through these points is called the K_f-line representing the transformed Mohr-Coulomb envelope.

Engineers often desire to depict successive states of stress that exist in a soil for the same initial conditions. Mohr circles may be drawn to depict each state of stress. As loading on a specimen is altered either through an actual construction sequence or in testing a specimen in the laboratory the states of stress vary significantly. A diagram representing these conditions can be quite confusing as the complexity of the system increases. A more satisfactory arrangement is to plot a series of stress points and to connect these points with a line or smooth curve (Figure 2.8). Such a line or curve is called a stress path. The stress path may depict total stress conditions or effective stress conditions. The respective stress paths are called Total Stress Path (TSP) and Effective Stress Path (ESP). Figure 2.9 shows the stress path of a normally consolidated Weald clay under triaxial testing. Many types of laboratory testing utilize $\sigma_1 = \sigma_3$ as the initial condition (14). Thus, the engineer has an efficient and effective tool to analyze stress distribution and evaluate the geotechnical properties of undisturbed and remolded soil.

Varved Clays

General

Engineers often consider clay and soil (in general) as a homogeneous isotropic material. In reality this is far from the case. In many locations, clay deposits are found in which the clay, being sedimentary in origin, exhibits a definite layered structure. Clay deposits,

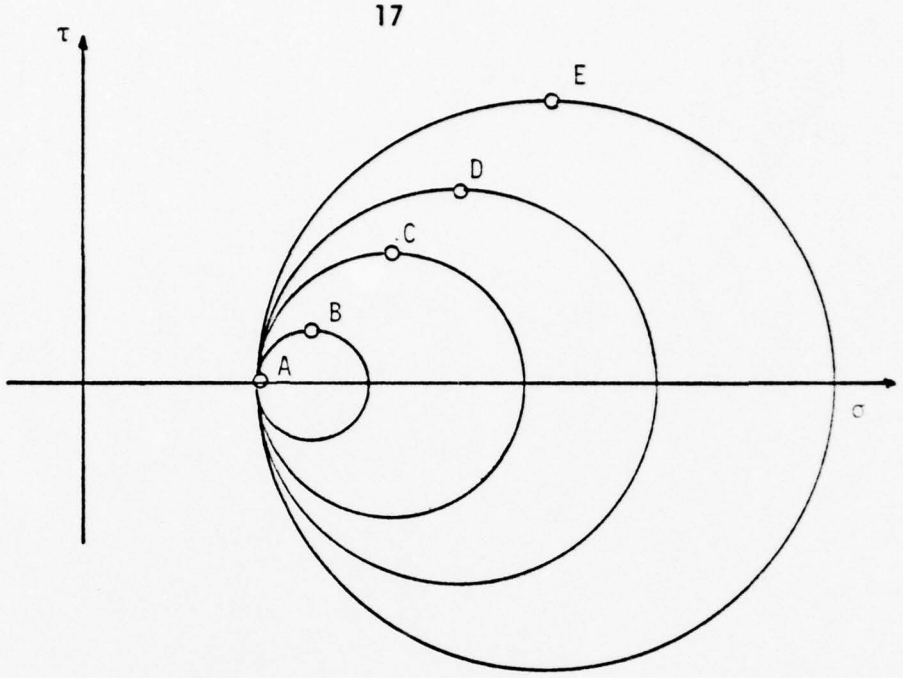

a. Mohr circles

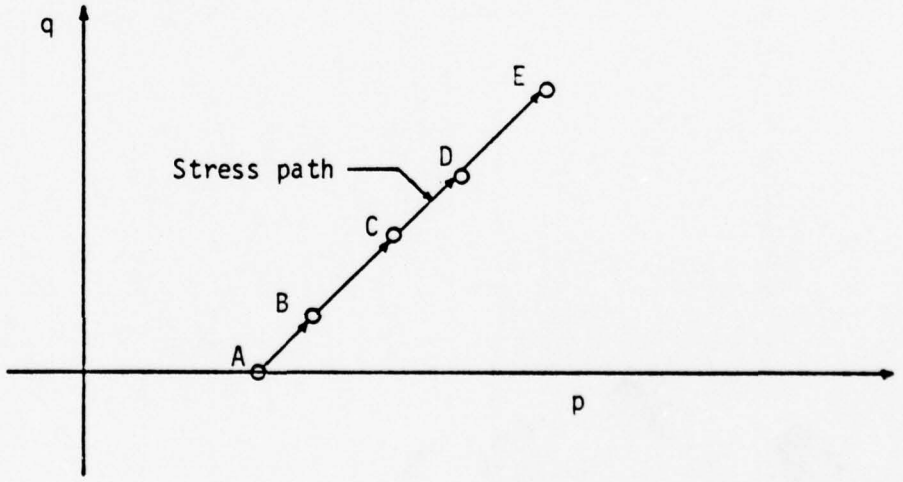

b. p-q diagram.

Figure 2.8. Representation of Successive States of Stress as σ_1 Increases with σ_3 Constant. Points A, B, etc., Represent the Same Stress Condition in Both Diagrams.

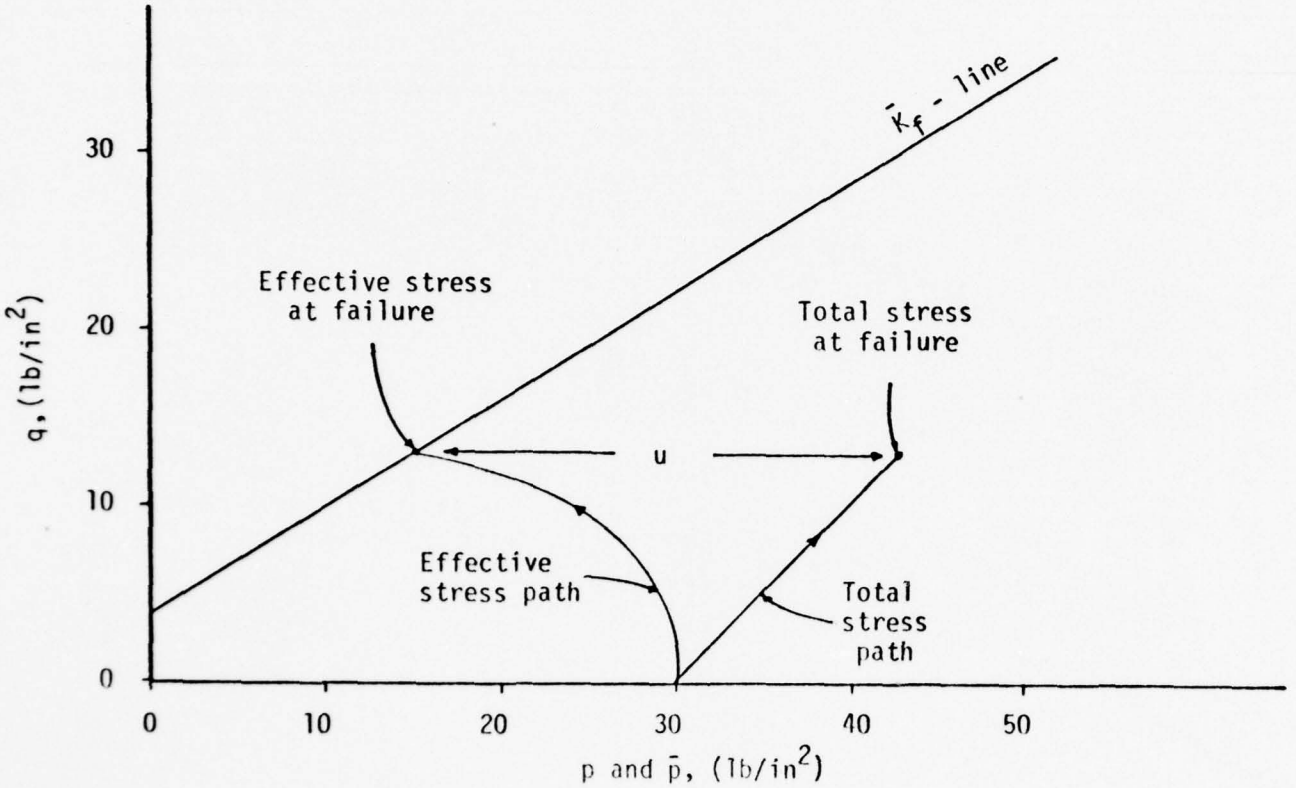

Figure 2.9. Normally Consolidated Weald Clay with $\bar{p}$ = 30 psi.

in which cyclic sedimentation has produced a repetition of layering or laminations and internal structure, have commonly been called "varved" clays (32). The geology and chronology of varved formations is open to some dispute. Many of these banded sediments are found in North America, Scandinavia, and the U.S.S.R. and have been attributed to diurnal, annual, and aperiodic variations in discharge of sediment load from glaciers. The term varve usually refers to annually deposited couplets of fine winter layers and coarser summer layers. However, marine sediments also display laminations of silt and clay that technically may be classified as varved.

Modes of Formation

There appear to be two primary modes of formation associated with banded sediments. The first mode is related to glacial activity in the northern hemisphere. The second mode is a function of precipitation variations in more temperate climates.

During periods of glaciation varved sedimentary deposits have formed as a result of the cyclic temperature changes associated with the seasons. The variation in stream flow is quite pronounced. The velocities of the streams emanating from the glaciers during the melt season, spring and summer, allowed only layers of coarser material to settle. With the onset of winter the water velocity slows and finer soil particles settle out. Another common characteristic of glaciation is the disruption of normal drainage patterns along streams and rivers. Blockades of ice or rock materials released by the melting ice form basin areas. These lake areas may last for hundreds of years and are

excellent sediment collection basins. While in existence, the lakes serve as catchment areas for the products yielded by normal weathering, erosion and stream transportation, as well as the variety of rock material released by the melting ice. The coarsest materials are deposited close to the stream mouth while the finer materials are dispersed throughout the lake water and gradually settle out. Silt size particles settle during the more turbulent water periods of spring and summer while the finer clay fraction settles chiefly during the winter. The variation of water velocity due to annual climatic changes produces the sharp demarcation between successive layers (27). The Columbia River Valley and its tributaries in north-central and northwestern Washington are noted for extensive varved deposits of this type (32). The topography of Canada also shows the existence of numerous glacial lake sources of lucustrine varved sediments. Canada has an abundance of varved clay deposits from both glacial streams and basins. The retreat of the last ice sheets in Scandinavia is recorded indelibly in the varved clay deposits (17).

Aside from the predominant glacial sediments familiar to engineers, large regions of the earth are exposed to recurrent variations in precipitation during wet and dry seasons. Under favorable conditions these variations are reflected in the erosion and deposit of sediment. Again, the seasonal activity is reflected in low and high stream flow. The great expansive plains in the western United States and South America show the non-glacial sedimentary patterns. These continental and coastal deposits come primarily from the predominant mountain ranges in the area such as the Sierra Nevada Mountains and the Andes Mountains.

Wave action, tidal forces and currents, and stream velocities all contribute to sedimentary deposits at the continent's edge. Many river areas at the perimeter of the large land masses have laminated deposits of clay and silt. The Port of Guayaquil, Ecuador is characteristic of non-glacial sedimentary deposits. This area is a mixture of tropical rainy and dry climates exhibiting definite periods of high and low precipitation (8). These areas were gradually exposed during the Tertiary Period of geochronology and have been developed recently as port facilities and population centers (27).

Geotechnical Properties

The documented engineering experience associated with varved clays is extremely limited. Literature concerning the detailed geotechnical properties of layered systems is therefore not extensive. A comprehensive work on experience with Canadian varved clays was presented by Milligan, Soderman and Rutka (1962) (17) in which specific case records were analyzed. A recent study of Parsons (1976) analyzes the glacial lake formations in New York as prospective construction sites (20).

One of the most significant properties of varved clays is its structure. Various theories have been advanced which define the behavior and nature of varved clay structure. The consensus explanation for the varved clay system is that the dispersed manner of deposition creates a flocculated soil structure (29). This "cardhouse" concept was first advanced by Goldschmidt (1926) (18) and is applicable to varved clay formations. The mode of formation is characterized by an

"edge-to-face" arrangement of particles similar to that of a cardhouse. Various electrolytes in the soil water have also influenced the dispersion of the system contributing to this type of soil fabric. X-ray diffraction of soft deposits of varved clay in the vicinity of New Liskeard, Ontario has substantiated the metastable nature of these clays (20).

The layered nature of the varved soils and their relatively sensitive structure has complicated the assessment of soil strength. The determination of the shear strength of the soil has been primarily confined to studies of the entire layered system and not to the individual laminations. A review of the literature shows that most studies on layered clays have investigated other engineering properties relating to consolidation and pore pressure. A macroscopic evaluation of shear strength characteristics, for particular soil types, is normally made simply for comparative analysis.

Undisturbed samples normally display a definite inclined failure plane that intersects a majority of the laminations (30). Pore pressure equalization will exist in the undrained testing. With the equalization of pore pressures the strength of the coarse layer (silt layer) is somewhat decreased while the strength of the fine layer (clay layer) is increased slightly. The effective stress parameters reveal that as the amount of fine material in the system increases the effective stress will decrease (29). The effective angle of internal friction $\bar{\phi}$ may also be dependent on the various bands of sediment. The clay phase normally has lower angles with higher liquid limits while the silt phase has higher angles with lower liquid limits. Variation in the thickness of layers

within the deposit is the prime cause for extreme variation in their properties (17).

The permeability of varved clays is not constant in all directions. The anisotropic nature of laminated systems allows for rapid pore-pressure dissipation, is vital in the analysis of stability problems and is critical in consolidation and settlement analyses. It is apparent that shear strength and related geotechnical properties are functions of individual layer thickness, the continuity of the layers and their relative structure (17).

Clay Sensitivity

General

Sensitivity is a phenomenon exhibited by virtually all normally consolidated clays (18). Sensitivity was first quantitatively characterized by Terzaghi (1944) who used the following relationship as determined from the unconfined compression test.

$$S = \frac{q_u}{q_{ur}}$$

where S = sensitivity ratio based on ultimate strength

q_u = unconfined compressive strength at failure of undisturbed sample

q_{ur} = unconfined compressive strength at failure of the remolded sample (30)

Clays that exhibit extremely low remolded strengths such that a specimen cannot be formed require shear strength measures using the vane shear test. Current techniques to evaluate sensitivity utilize undrained

strengths as determined by triaxial testing for specific conditions; i.e., peak value strength or a given vertical strain.

Problems involving slope stability and settlement have prompted extensive studies of sensitive clays. The post-glacial clays of Scandinavia and Canada have varying degrees of sensitivity. Clays that lose all shear strength with outside disturbance, called "Quick Clays," are common in these areas. The causes of clay sensitivity are not completely understood. Mitchell (19) has made a comprehensive study of the mechanisms which may contribute to the significant loss of strength with remolding.

Causes of Sensitivity

With the aid of advanced technology it has been determined that at least six different phenomena contribute to the development of sensitivity.

1. Metastable Fabric
2. Cementation
3. Weathering
4. Thixotropic Hardening
5. Leaching, ion exchange and change in monovalent/divalent cation ratio
6. Formation or addition of dispersing agents

1. Metastable Fabric

The arrangement of particles and particle groups in any fine-grained soil is critical to its geotechnical properties. Sedimentary soils are arranged in various flocculated arrangements capable of

carrying substantial loads (Figure 2.10). Destruction of the rigid framework through remolding causes a loss in effective stress, change in volume and reduction in overall strength.

2. Cementation

Investigations by Bjerrum and Wu have shown that after sedimentation, bonds between particles are formed that have the characteristics of chemical cementation compounds. The cementing agents such as free carbonate, alumina, organic matter and iron oxide may precipitate onto the interparticle contacts during formation. This glue forms a rigid bond between particles creating a relatively strong lattice resulting in additional resistance to compression (4).

3. Weathering

Weathering processes control the flocculation-deflocculation tendencies of soil. The presence of various ions and their proportions in solution control the expansion and contraction of the diffuse double layer subsequently affecting interparticle forces. Strengths and sensitivities may be increased or decreased depending on the nature of the charges in ionic distribution. The mineralogical composition and grain size distribution resulting from the weathering process will influence the development of different fabric types.

Moum and Rosenqvist have studied the effects of weathering on illitic clays originally saturated with sodium ions. During the weathering of surrounding materials potassium ions replace the sodium. This has resulted in increases of both undisturbed and remolded strengths (19).

Deflocculated, dispersed

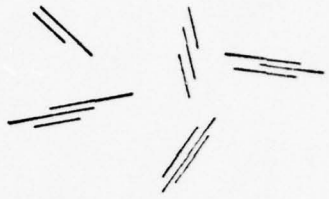

Deflocculated, aggregated

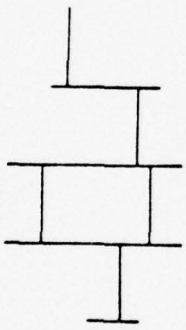

Edge-to-face flocculated, dispersed

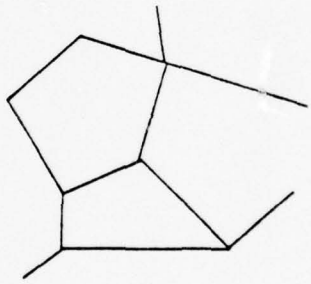

Edge-to-edge flocculated, dispersed

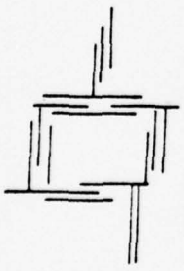

Edge-to-face
Flocculated, aggregated

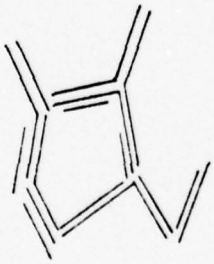

Edge-to-edge
Flocculated, aggregated

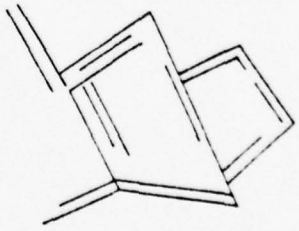

Edge-to-edge & edge-to-face
Flocculated, aggregated

Figure 2.10. Clay Particle Assemblages

4. Thixotropic Hardening

Thixotropy is defined as a time dependent process whereby a material stiffens and gains strength while at rest, and softens upon remolding. A fabric change occurs with remolding resulting in a deflocculated state. While a certain amount of externally applied energy exists on the system it remains in equilibrium as a liquid. With removal of the external energy, the interparticle forces of attraction tend to reflocculate the aggregate of particles. The reorganization causes an increase in the strength of the material. Though some remolded laboratory specimens have displayed this characteristic, little is presently known concerning the effect of thixotropy in field conditions (18).

5. Ion Exchange

Rosenqvist (1946) first suggested that sensitivity may develop by changing or eliminating ions in the soil water. The leaching of sodium from marine clays is an essential step in the development of quick clays (19). Washing of the soil by relatively pure water either through percolation or the lifting of clay layers above sea level will cause a reduction in ion concentrations. The leaching effect causes little disturbance in the fabric and primarily influences the interparticle forces. A large increase in interparticle repulsion through a decrease in electrolyte concentration will normally exist, causing a significant loss of remolded strength. Studies have shown that sensitivity correlates well with the percentage of monovalent cations in the pore water (18).

6. Dispersing Agents

Some highly sensitive clays are found in the vicinity of organic layers such as peat. Organic compounds also exist in the pore water during formation of the sediment. Some of these substances, often acidic in nature, act as dispersing agents and cause increased double layer repulsion. The fabric that is formed is similar to the marine sediments. Due to the complexity of the organic compounds, their full effect on sensitivity is not yet clear (18).

Though various mechanisms contribute to sensitivity, the fundamental cause of sensitivity in clays is the change in fabric which occurs from external disturbance and remolding. It is understood that a flocculated arrangement of clay and silt particles develop a more rigid framework with high load-carrying ability than the same particles arranged in a deflocculated manner at the same water content. Characteristics of the above mechanisms are summarized in Table 2.1.

Physical Property Interrelationships

Extensive clay sensitivity studies (18, 16, 30) have resulted in the development of relationships to describe the varying degrees of sensitivity in clays. The relationships that have been shown as most reliable are those of sensitivity, liquidity index and effective stress. An understanding of these factors can alert the engineer to impending geotechnical problems and allow for a better understanding of site conditions.

Table 2.1. Causes of Clay Sensitivity

Mechanism (1)	Type of reaction (2)	Limit of sensitivity (3)	Predominant soil types affected (4)
Metastable particle arrangements	Physical	Slightly quick[a] (8-16)	All clays
Silt skeleton-bond clay	Physical	Very sensitive (4-8)	Clay-silt-sand mixtures
Cementation	Chemical	Slightly quick (8-16)	All soils containing potential cementing compounds
Ion exchange	Physico-chemical	Slightly quick (8-16)	Leached and weathered clays
Leaching of salt	Physico-chemical	Extra quick (64)	Glacial and post glacial marine clays
Weathering	Chemical	1.0 to Medium sensitive (1-4)	All soils-magnitude of effect depends on mineralogy
Thixotropic hardening	Physico-chemical	Medium sensitive to slightly quick[b] (2-16)	Clays
Dispersing Agent addition	Physico-chemical	Extra quick (64)	Clays-particularly organic bearing or organic deposit associated

[a]According to Rosenqvist scale.

[b]Pertains to samples hardening starting from present composition and water content. Role of thixotropy in causing sensitivity of clays *in situ* is indeterminate.

Sensitivity and effective stress parameters have previously been defined. Liquidity index (LI) uses basic soil properties as a comparison of degrees of sensitivity.

$$LI = \frac{(w - PL)}{(LL-PL)}$$

w = Water Content

LL = Liquid Limit

PL = Plastic Limit

Mitchell used the considerable data in the literature for various soils to establish the general relationships between sensitivity-effective stress and liquidity index for all clays. The contours found in Figure 2.11 depict these relationships. Although this graph may not be accurate for all clays, it is a useful tool for the engineer (9).

Several other properties have been found to associate well with the sensitivity of clays. The activity (plasticity index/clay fraction) generally has been found to decrease with increasing sensitivity. The ratio of undrained shear strength (defined as half the maximum deviator stress) to consolidation pressure, C/p, generally decreases with increasing sensitivity. In general, sensitive clays have lower values of vertical strain at failure as a result of the brittleness of the material and susceptibility to fracture (9).

The value of the pore pressure parameter A has been useful in the classification of soils. When an increment of stress is applied to a confined saturated sample of soil there is a corresponding increment

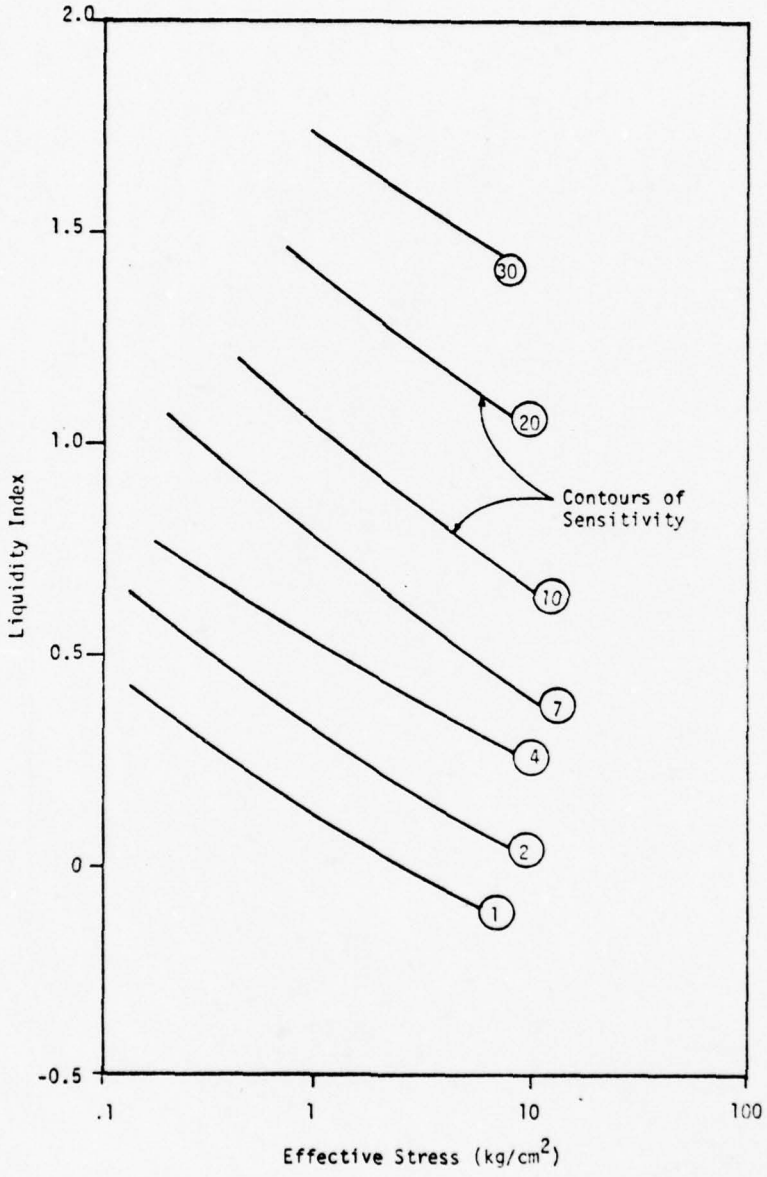

Figure 2.11. General Relationship between Sensitivity, Liquidity Index, and Effective Stress.

of pore pressure built up. The direct way to determine this relationship is through the parameter A (24).

$$A = \frac{\Delta u - \Delta\sigma_3}{\Delta\sigma_1 - \Delta\sigma_3}$$

In the usual undrained conditions of the triaxial test $\Delta\sigma_3 = 0$ and the relationship reduces to

$$A = \frac{\Delta u}{\Delta\sigma_1}$$

It has been found that this parameter is not a constant soil property. Typical values given by Bjerrum (14) for A at failure show sensitive clays have a range of 1.5 to 2.5, where normally consolidated clays vary between 0.7 to 1.3. The value of A may conveniently be determined graphically from the $\bar{p}$, $\bar{q}$ diagram using the effective stress path and $\bar{K}_f$-line. Caution should be used in depending significantly on A values from the literature. This parameter depends strongly on the particular stress conditions under consideration. The engineer should conduct tests to determine the particular pore pressure parameters to be used in estimating pore pressure changes in the field (14).

Closure

Varved clay is an important geotechnical material with limited engineering information available. As indicated previously, most experience with varved clays is in the northern hemisphere. Analysis of varved systems in the southern hemisphere is practically non-existent.

The combination of a varved clay system with the possibility of a sensitive structure further complicates the situation.

The information contained in this study will focus on a varved sedimentary deposit on the west coast of South America. Testing this important geotechnical material will provide some insight into the various engineering properties necessary for a thorough understanding of soil behavior. The evaluation of data obtained from testing undisturbed samples of this material will provide specific parameters necessary for analysis and design of earth structures. Shear strength comparisons will be made between undisturbed and remolded specimens, and the sensitivity evaluated. A general mineralogical composition will be formulated and phase relationships measured.

III. EXPERIMENTAL PROCEDURES AND EQUIPMENT

The specific methodology to permit a quantitative definition of macroscopic soil properties is presented. The consolidated-undrained form of the triaxial compression test was used to provide the representative data to evaluate the complex soil properties of an Ecuadorian varved clay. The triaxial testing and data collection equipment used to define the shear strength characteristics of the soil are described. X-ray diffraction and thermal gravimetric analysis procedures were used to define the mineralogical composition of the Ecuadorian soil. A brief description of these soil testing techniques is also presented.

Testing Theory

General

The object of laboratory testing is to model field conditions as closely as possible and through this modeling evaluate sufficient parameters for analysis and design. The consolidated-undrained compression test (CU) provides the necessary flexibility in achieving in situ conditions for this particular clay soil being studied. There are various modes for applying states of stress associated with the triaxial test. Under conditions usually encountered in the field, the low permeability of saturated clay greatly retards drainage; as a consequence, the pore pressures associated with the stresses tending to shear the clay may not dissipate readily. It must be noted that this is not a long term

condition. Gradual dissipation of pore pressures will exist during and after the construction sequence. This non-drainage condition may be approximated in the CU triaxial test (28). This test also allows for the application of similar stress conditions experienced in the field during the construction sequence. Through the measurement of pore pressure during these various stress states the shear strength parameters may be obtained in terms of total and effective stresses. The additional flexibility inherent in the CU test provides insight into the structure and true shear resistance associated with saturated cohesive soils.

Consolidated-Undrained Triaxial Test (CU)

The standard consolidated-undrained test is a compression test in which the soil specimen is first consolidated with an equal all around pressure. Failure is then brought on by increasing the major principal stress (3). Figure 3.1 shows the actual sequence of steps in the CU test. In this figure, u_r, denotes the residual pore pressure after sampling of the soil. This is a negative pore pressure associated with capillary tension and the releasing of the in situ stress condition. During the consolidation phase, step 2, drainage is permitted and pore pressures dissipate to zero. Upon completion of primary consolidation the axial stress is increased until failure, step 3. Pore pressure build up will occur since the specimen is not allowed to drain during this final phase. The measurement of pore pressure during steps two and three permit determination of the effective stresses existing during

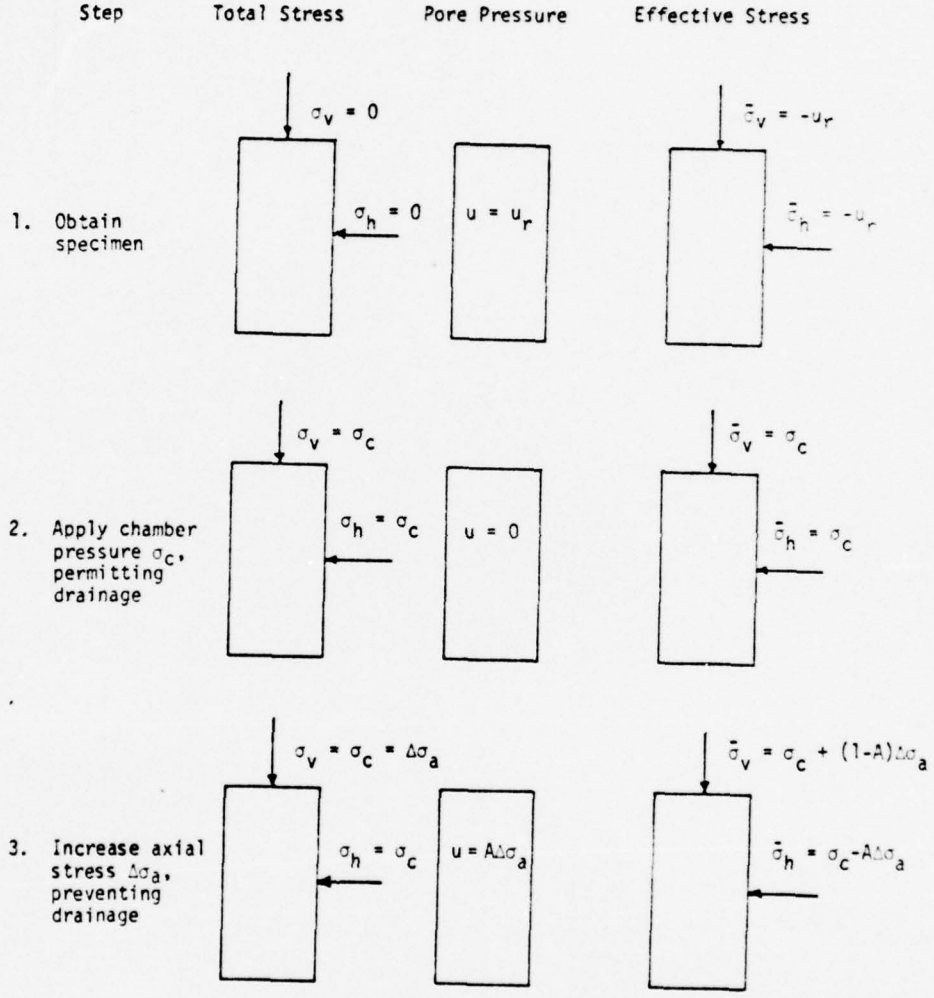

Figure 3.1. Consolidated-Undrained (CU) Triaxial Test.

undrained loading and leads to an understanding of the relationships between undrained and drained strength (14).

Pore Pressure Parameters A and B

In 1954 Skempton introduced the concept of pore pressure parameters to explain how the pore pressure responds to the different combinations of applied stress. This concept may be expressed by the following equation:

$$\Delta u = B[\Delta\sigma_3 + A(\Delta\sigma_1 - \Delta\sigma_3)]$$

This expression does not take into account the value of the intermediate principal stress. However, empirical evidence has shown that Skempton's model applies quite well to the triaxial compression test since in this experiment $\sigma_2 = \sigma_3$. The derivation of these parameters is essentially based on the incompressibility of the pore water and soil particles and the compressibility of the soil skeleton. A complete derivation may be found in reference (24).

As indicated in Chapter 2 the parameter A is far from unity. It is a vital parameter for predicting soil conditions and pore pressure changes in the field. The evaluation of this parameter and the measurement through triaxial testing is the same as indicated previously.

For fully saturated soils, the parameter B = 1 within experimental accuracy and may be expressed by the relationship

$$\Delta u = B\Delta\sigma$$

This is the pore pressure developed by an increment of isotropic stress through three dimensional loading. It is essential that this relationship hold during triaxial testing. Thus, it is necessary to insure that undistrubed samples are 100 per cent saturated. Insuring this degree of saturation allows for accurate measurement of pore pressure build up during the loading phase (3). The technique of back pressuring the specimen insures values of $B \simeq 1$, by filling all voids with water and dissolving gases in the soil specimen.

Instrumentation

General

The three major items necessary for obtaining the required data associated with the three phases of the CU test are 1) the triaxial cell, 2) the volume change apparatus, and 3) the pore pressure measuring devices. Our system is further refined, compared to most commercial laboratory testing equipment, by a data acquisition and recording system. All pressure and deformation functions are monitored by electrical transducers. All data were monitored by a data acquisition system providing a digital display and printout.

The Triaxial Cell

The triaxial cell (Wykeham Farrance Model 17038M) used in this experiment is a low pressure (1200 KN/m^2 chamber pressure) cell manufactured from light alloy, noncorrosive material by Wykeham Farrance Limited, England. The cell is designed to accommodate 70 mm diameter samples but may be modified for other specimen sizes. The base pedestal is drilled with two holes which can be used for bottom drainage, back

pressure or flushing purposes. Four ducts are drilled in the cell base, all of which lead externally to no-volume-change valves. Two of these ducts connect with the pedestal holes. One of the remaining ducts is used for filling and emptying confining fluid in the chamber. The last duct provides a connection for top drainage or for back pressuring through the specimen top cap. To provide maximum visibility, the cell chambers are made from perspex (lucite) which is stress relieved during manufacturing.

The loading mechanism is unique to this triaxial cell. Most triaxial cells use a solid steel shaft to transfer load from the proving ring and load frame to the specimen in the chamber. This particular cell contains a load transducer designed for mounting internally in the triaxial chamber. The load cell replaces the proving rings and dial gages and eliminates the ram friction that was formally included in measurements. The load cell is so designed that it is insensitive to hydrostatic pressure and eccentric load. Electric signals generated by strain gages mounted within the fluid immersible transducer provide instantaneous measurement of the applied load (Figure 3.2).

Volume Change Apparatus

The automatic volume change apparatus (Wykeham Farrance Model 10938) is a significant advancement in the monitoring of triaxial and consolidation tests in the laboratory. With the advent of the electronic linear variable displacement transducer (LVDT), the change in specimen volume occurring in the drained stage of the triaxial test could be

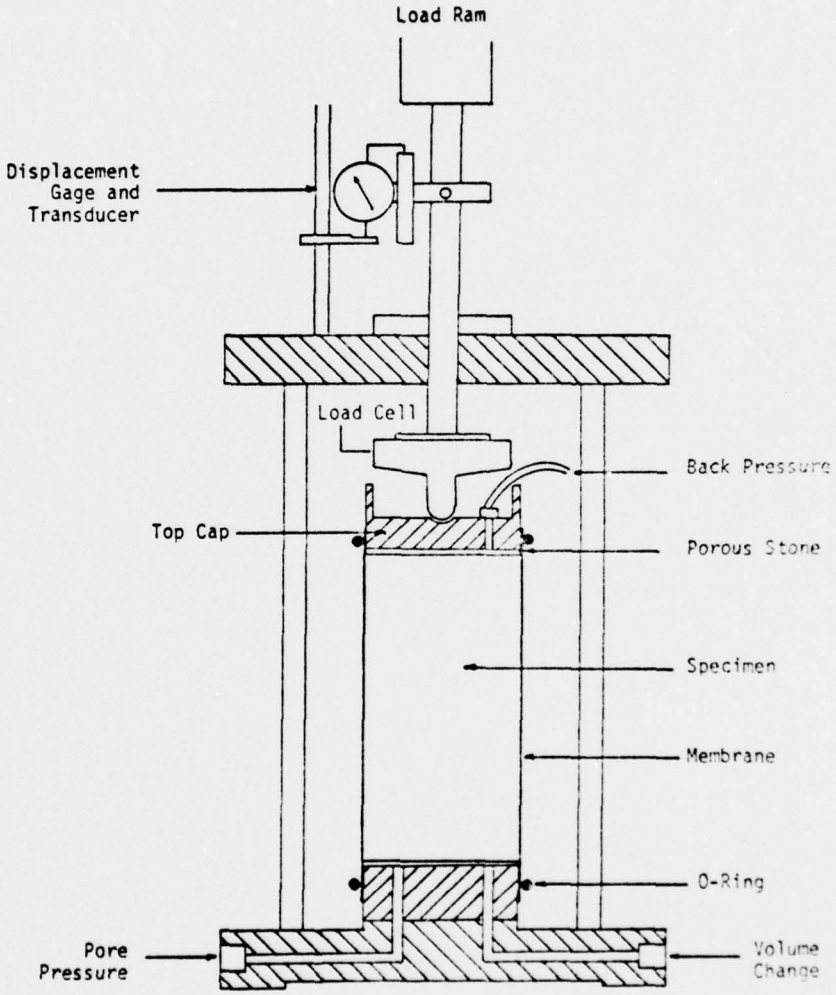

Figure 3.2. Triaxial Cell

easily measured. The device gives a sensitive measurement of volume change and is suitable for automatic data acquisition.

The LVDT consists of a vertical concentric clear perspex tube clamped between horizontal end plates. A short inner perspex tube is separated into an upper and a lower chamber by a brass piston incorporating a Bellofram rolling diaphragm. The armature of a water-submersible displacement transducer is connected to the piston. The device is filled with de-aired water. The valve system is connected to the triaxial cell pore water duct and a constant pressure source. Any displacement of water in the duct will cause a corresponding displacement of the piston. Reversing the valves on the panel continuously extends the capacity of the device by changing the direction of the piston. An LVDT may be calibrated so that sensing the transducer output provides direct volume change (cc) output on the acquisition system (Figure 3.3).

Pore Pressure Transducers

The perfection of pore pressure transducers has further simplified the recording of data from the triaxial test. The general purpose transducer converts the fluid pressure exerted on its diaphragm into an electrical signal via an excited Wheatstone bridge. The transducer has an all welded case of stainless steel. The flush diaphragm type of construction allows for negligible volume change while sensing the pore water pressure. The output is a linear function of the pressure applied to the diaphragm and can easily be calibrated to read directly in the desired units.

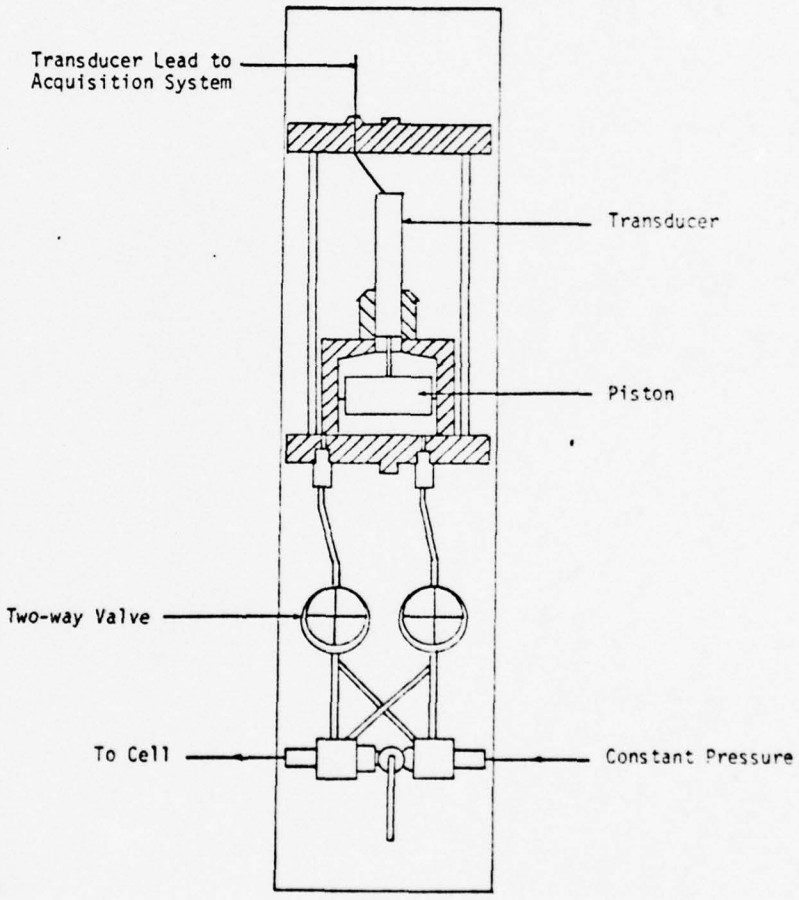

Figure 3.3. Volume Change Apparatus.

Data Acquisition System

The data acquisition system (Troxler Electronic Laboratories Model 13830) used in this experiment is a solid state electronic modular instrument for the collecting and recording of data from measurement transducers. The transducers convert the mechanical measurements of pressure and displacement into an electrical signal which is proportional to the measurement. Each input in turn is connected to its individual conditioning module which provides an output easily related to the measurement.

Triaxial testing requires the simultaneous reading of several soil measurements over varying periods of time. Unique to this system is the ability to read information at regular intervals of time from a number of measuring points. In the automatic scan mode, the scanner sequentially scans all the inputs, so designated through a manual skip/scan switch, in rotation, on a time base. Each measurement is displayed on the panel meter in a numerical form and simultaneously printed on paper tape for a permanent record. In the manual mode, individual channels may be monitored as desired during the sequence of testing. The versatility of this system allows for several types of experiments to be conducted at the same time at varying intervals of time. As an example, during the consolidation phase, the acquisition system may be programmed to read and print pore pressure dissipation and volume change at time intervals proportional to the square root of time. Thus the recorded data may be easily plotted to obtain standard volume change-elapsed time curves.

Sample Preparation

Undisturbed Samples

Soil Samples were obtained from Guayaquil, Ecuador following as closely as possible the technical provisions of ASTM D 1587-67. At a desired sampling depth, a 30 inch long section of 16 gage, 3 inch O.D. steel tubing was hydraulicly advanced into the soil. Once the sampling tube was carefully removed, the ends were sealed in micro-crystalline wax and placed in a protective container for shipment to the Geotechnical Engineering Research Laboratory at Auburn University (34).

Once the testing sequence began, individual boring tubes were placed in the extruding machine and securely clamped. Procedures described by Hvorslev (10) were followed to minimize the sample disturbance. Each end of the tubing was cut using a fine tooth hacksaw blade and the wax removed. Burrs and any obstructions were removed to insure a smooth sample and reduce resistance. A tight fitting piston was placed in the tube and a steady pressure forced the sample onto a lubricated semicircular trough for further handling. Due to the relatively short length of the tubes the samples were extruded as a unit. The unit was subdivided into desired lengths for full specimen (70 mm diameter) testing, wrapped in PVC wrap, sealed in paraffin and stored in a high humidity environmental chamber until required.

Remolded Samples

Test specimens for the remolded shear strength determination were obtained from samples prepared in a modified consolidometer as outlined by the Waterways Experiment Station (WES) (7). A mixture of

de-aired, demineralized water and undisturbed soil were blended forming a slurry. This slurry was de-aired and then poured into a length of sampling tube sealed at one end with a porous stone. Another porous stone was placed on top of the slurry to allow pore water drainage. A consolidation pressure approximating the in situ geostatic pressures was used. Since pore water pressure could not be applied to specimen during the consolidation as in the WES design, difficulty was encountered in obtaining consistent water contents. For testing purposes water contents that would provide a sample capable of standing under its own weight were used.

Triaxial Specimen Preparation

Individual test specimens were trimmed from the samples so that the vertical axis of the specimen was parallel to that of the sample. Trimming was kept to a minimum for the undisturbed samples. Moisture contents were determined using the trimmings and compared with the boring logs to estimate any moisture loss which occurred during storage. No significant moisture losses were identified. Each specimen was cut to a minimum of 2:1 length-diameter ratio and placed on a saturated porous stone covered by a filter paper (Whatman No. 1) disk on the pedestal of the triaxial cell. The filter paper between the soil specimen and porous stone prevented migration of fines and resultant obstruction of drainage and measuring ports. A moistened filter strip (Whatman No. 54) cage as described by Bishop and Henkel (3) was placed around the specimen. However, work by the WES has shown that if the cage extends the full length of the specimen, pore pressure measurements during the

saturation phase of the test would reflect the response of the strips rather than that of the specimen (35). For this experiment the filter cage covered 75 percent of the specimen periphery. After placement of the upper porous stone and filter disk, the specimen was encased in a standard rubber membrane. The bottom of the membrane was secured to the pedestal with two O-rings. After the top cap was placed on the porous stone, the membrane was rolled up the cap and smoothed out, again securing with two O-rings. Once the tubing from the top cap was fastened to the back pressure duct on the pedestal base, a vacuum was applied to remove any entrapped air. The perspex chamber was secured to the base and allowed to fill with a confining fluid of blended de-aired, distilled water and glycerine. This mixture consisted of two parts glycerine and one part distilled water.

Testing Procedures

Saturation Under Back Pressure

The back pressuring technique suggested by Dr. Frank C. Townsend, Waterways Experiment Station (35) was used. Although the specimens were essentially saturated prior to testing, this procedure insures a B coefficient close to one and also insures saturation of the measurement system.

When air ceased to flow from the specimen during the vacuuming or de-airing process, de-aired water was allowed to flow back into the specimen while simultaneously decreasing the vacuum and increasing the chamber pressure to 30 kN/m^2. This pressure was maintained as a differential pressure (chamber pressure minus back pressure) throughout the

saturation phase. To insure that the specimen was not significantly pre-stressed during the saturation phase, the back pressure was applied in small increments of 69 kN/m^2, with adequate time between increments to permit equalization of pore water pressure throughout the specimen. With the valves closed to the chamber and specimen, pressure increases of 69 kN/m^2 were preset on the regulators insuring that the original differential pressure was maintained. The preset pressures were then applied simultaneously to the chamber fluid and specimen. The pore pressure was measured at the base of the specimen and the parameter B evaluated immediately upon application of each increment. The pore pressure was observed until it became essentially constant. Increments were continually added until, under any increment, the pore pressure reading was equal to the applied back pressure immediately after opening the valves. Verification of the completeness of saturation was made by keeping the valve to the top of the specimen closed and incrementally increasing the chamber pressure. If the pore pressure response was immediate and equal to the increase in chamber pressure the specimen was ready for the consolidation phase (35). The back pressuring phase normally took 24 hours before B was essentially equal to one with the total applied back pressure being approximately 550 kN/m^2 (Figure 3.4).

Consolidation

All specimens were consolidated under an isotropically applied chamber pressure. When the specimen was completely saturated, the maximum applied back pressure was held constant and the chamber pressure was increased until the difference between the chamber pressure and back

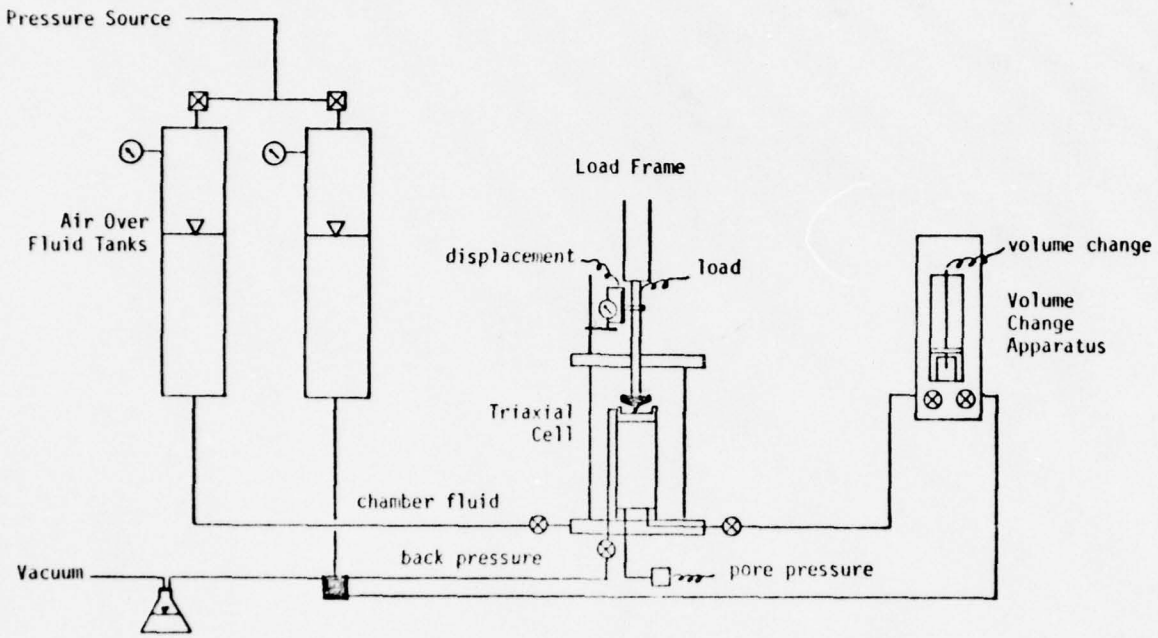

Figure 3.4. Triaxial Test Equipment Schematic.

pressure equaled the desired confining pressure (consolidation pressure), under which the strength determination was to be made. The specimen drainage valve was opened to the automatic volume change apparatus and the soil was allowed to consolidate. The data acquisition system was started with the automatic scanner set to read volume change at $\sqrt{t}$ intervals. Pore pressure dissipation was also observed in the manual mode during the consolidation phase. A plot of the readings and measurements versus the square root of time was made easily from the printout. Consolidation was allowed to continue until a marked reduction had been achieved. Normally, several subsequent readings were taken from this point to insure that the primary consolidation was achieved and the specimen was prepared for axial loading.

Shear

Upon completion of consolidation, the drainage valve was closed, and the specimens were axially loaded at a constant-rate strain. The rate of strain was sufficiently slow to allow pore pressure equalization throughout the specimen. Pore pressure readings from the top and bottom indicated a negligible gradient that was acceptable within experimental accuracy and load frame limitations. The specimens were deformed to approximately 20 percent vertical axial strain or to the point at which ultimate conditions were reached after failure. Pore pressure, load and axial deformation were recorded automatically at specific intervals of time by the acquisition system throughout the entire loading phase. Once the test was completed, the specimen was taken from the cell and the membrane and filter cage removed. The specimen was sliced

horizontally, and water contents of the slices were determined. Constant water content throughout the specimen indicated equalization of the pore pressure.

Clay Mineral Identification

Two analytical techniques for the qualitative identification of the layer-silicate minerals present in the soil samples were used. X-ray Diffraction was the primary method, while Thermogravimetric Analysis was used to approximate the amount of kaolinite and gibbsite (36).

X-ray Diffraction

X-ray diffraction techniques utilize the principle of Bragg's Law, $n\lambda = 2d \sin \theta$, in which the distance, d, between crystal planes can be calculated if the angle of diffraction, θ, and the wave length, λ, of the X-ray beam are known. n is the order of reflection. The minerals present can be identified from the diffraction pattern since each type of clay mineral has unique crystal spacing. Quantitative determination of the amounts of different minerals is not normally done through this method.

The clay fraction (particles finer than two microns) was deposited on filter paper using a millipore apparatus and vacuum. During the filtration process different samples were treated to aid in identification. One set of a particular sample was potassium saturated while the other set was magnesium saturated and glycerol solvated. Glycerol expands the montmorillonite. Heating of the potassium saturated sample will collapse any vermicullite present. After removing the millipore filter paper, the clay-side was placed on a clean glass X-ray slide and

gently rolled with a glass tube. The filter paper was slowly peeled off the slide leaving a uniformly distributed specimen with (001) plane orientation. The excess clay on the filter paper was retained for thermal analysis.

The X-ray pattern was obtained by scanning each slide with a copper X-ray source (λ = 1.541Å) produced by a Norelco X-ray tube. The intensity of the X-rays reflected from the sample were recorded as a function of the scanning angle θ. The θ values at the peaks were then converted to d-spacing values and compared against various references identifying the specific minerals (4, 18).

Thermogravimetric Analysis (TGA)

The loss of the hydroxyl ion, at different temperature ranges, allows for the quantitative determination of certain soil minerals. The characteristic weight loss of both gibbsite and kaolinite is valuable in approximating the amount of each mineral. Gibbsite loses 32 percent of its weight at temperatures from 257°C to 320°C, while kaolinite loses 14 percent of its weight between 350°C and 800°C.

A portion of the magnesium saturated clay fraction was placed in the DuPont 951 thermogravimetric analyzer and heated from 25°C to 800°C. The weight loss as a function of temperature was recorded and plotted by the DuPont 990 Recording Console. Using the above temperature ranges, the actual weight loss was obtained and the amounts of gibbsite and kaolinite approximated closely.

$$\text{e.g.} \qquad \%\ \text{Kaolinite of clay fraction} = \frac{\%\ \text{weight loss}}{.14}$$

IV. TEST RESULTS

A complete description of the Ecuadorian varved soil is presented, including the grain size distribution, Atterberg limits, and clay mineralogy. Deviator stress-axial strain behavior and deviator stress-pore water pressure behavior of undisturbed and remolded specimens are presented. A comparison of shear strength parameters obtained for undisturbed and remolded samples is included also.

Soil Description

Location

The soil tested in this study was a normally consolidated, sedimentary deposit located in the port expansion site of the Port of Guayaquil, Ecuador, latitude 2°16 S, longitude 79°53 W. The location of the borings was on the north bank of the Cobina estuary in an area approximately 1000m x 500m due east and adjacent to the existing port facilities. The area is primarily a mangrove swamp with the average elevation being 16m above sea level. The soil samples were cataloged according to their boring log number. All tested samples were taken from representative areas along the proposed construction site (Appendix).

Specimen Properties

Visual inspection of the extruded specimens indicated that the soil was essentially the same throughout the port expansion area. All

samples were greenish-gray in color. Further analysis indicated that the soil was a clayey silt with very fine sand/silt laminations approximately 1/16" to 1/8" thick and spaced at intervals of 1/4" to 1/2". The specimens were all classified as ML according to the Unified Classification System. However, because of the inherent disturbance of the soil in evaluating the Atterberg limits, these phase relations are considered as only generally representative of the in situ soil behavior.

The soil specimens were essentially 100 percent saturated upon extrusion and possessed high natural moisture contents and void ratios. The specific gravity for all specimens was 2.69. The liquidity index was also calculated as an indication of the possible sensitive nature of the soil. Table 4.1 shows the characteristic classification properties for each of the samples.

Due to the extremes of these fundamental properties, construction site difficulties would be expected. Void ratios greater than one normally create problems since the volume of void spaces (equal to the volume of water in the completely saturated condition) is greater than the volume of the soil solids.

The soil specimens displayed a stable nature prior to testing. They were relatively stiff and could be handled with little deformation. The fact that these specimens have a rigid nature upon extrusion but possess significantly high void ratios and moisture contents is indicative of a specific soil particle integrity and structural stability in an undisturbed state. This is the first indication that a specific soil fabric does exist for this soil.

Table 4.1. Soil Properties

Sample	Natural w%	LL%	PL%	PI%	Wet Unit Weight KN/m^3	Particle Size %			Void Ratio	LI
						Sand	Silt	Clay		
B3, M9	95.4	73	58	15	7.38	5.5	46.8	47.7	2.6	1.5
B5, M2	115.3	122	59	63	6.42	.2	57.4	42.4	3.1	-.11
B6, M4	106.8	82	49	33	6.82	2	53.1	44.9	2.9	.75
C3, M4	120	69	45	24	6.29	2.5	34.8	62.7	3.2	2.13

Mineralogy

The X-ray diffraction patterns and TGA results for the three samples are shown in Figures 4.1 through 4.5. These patterns show the identifiable minerals of the clay fraction. Each of the samples had identical reactions to the various treatments. As a result all samples are considered to have come from the same soil material.

The magnesium saturated patterns (Figure 4.1) show the characteristic basal spacings for smectite (montmorillonite) minerals, 12 to 15 Å; the hydrous mica (illite) minerals, 10 Å, and kaolinite minerals, 7.2 Å. The expansive characteristic of smectite after glycerol treatment provides for the positive identification of this mineral. Smectite expands to a basal spacing of 17 to 18 Å. The intensity of these peaks further emphasizes the dominance of this mineral in the soil.

The potassium saturated pattern shows the same characteristic patterns observed above. The heating treatment provides further identification of the minerals present. Upon heating to 300°C, smectite is destroyed. Further heating to 500°C will destroy the kaolinite minerals, leaving the fairly intense 10 Å illite peak which remains fixed throughout the treatment process.

Thermogravimetric Analysis was used to obtain the quantities of kaolinite and gibbsite present. The thermal reactions observed indicated the removal of water located in and around the clay minerals. The adsorbed water or water of hydration is driven off in the 100°C area. Further heating causes crystal lattice water in the form of (OH) ions to be expelled. The temperature at which the major amounts of crystal lattice water is lost is an indicative property for the identification

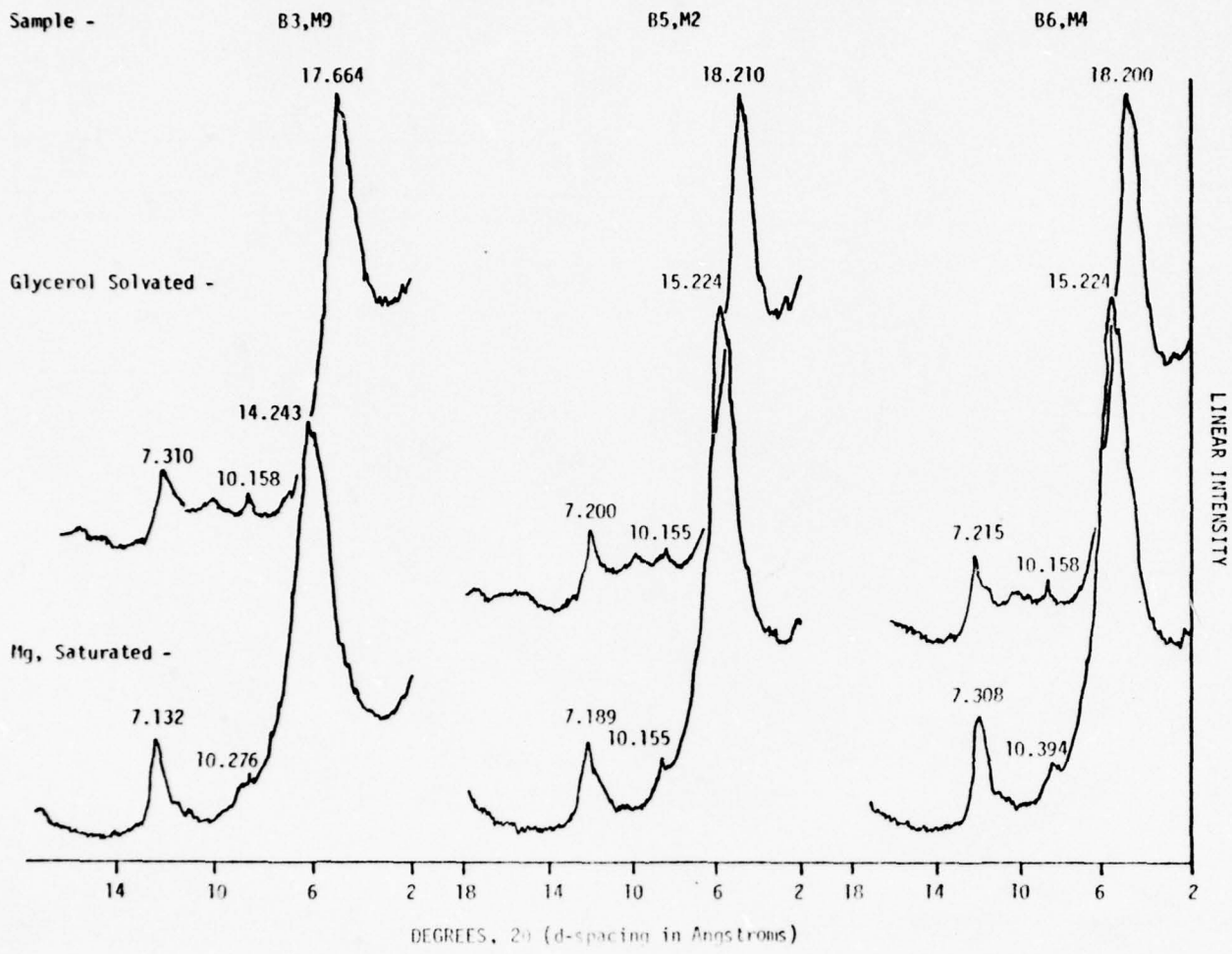

Figure 4.1. X-ray Diffraction Patterns, Glycerol Treatment

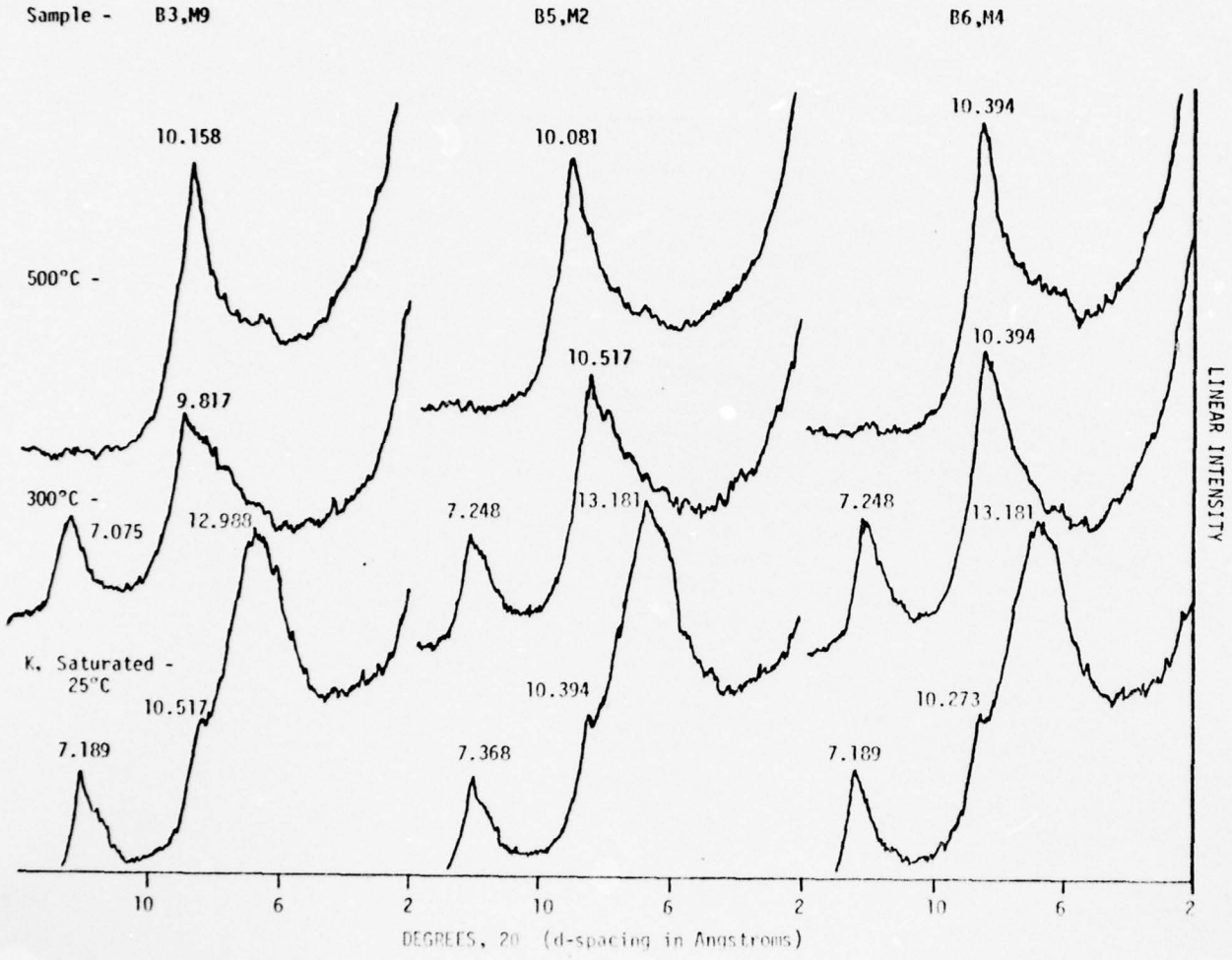

Figure 4.2. X-ray Diffraction Patterns, Heat Treatment

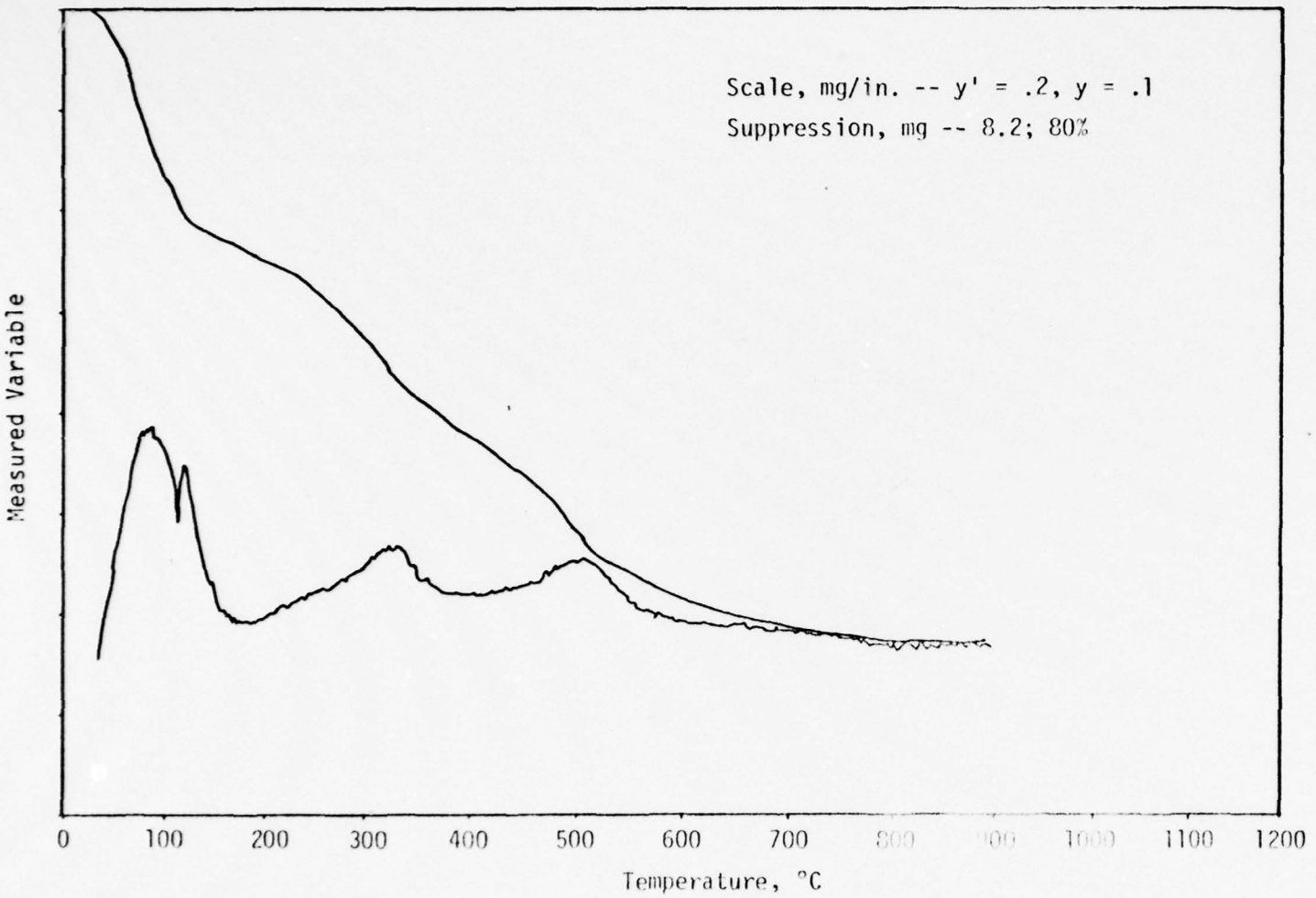

Figure 4.3. TGA Pattern, Sample [illegible].

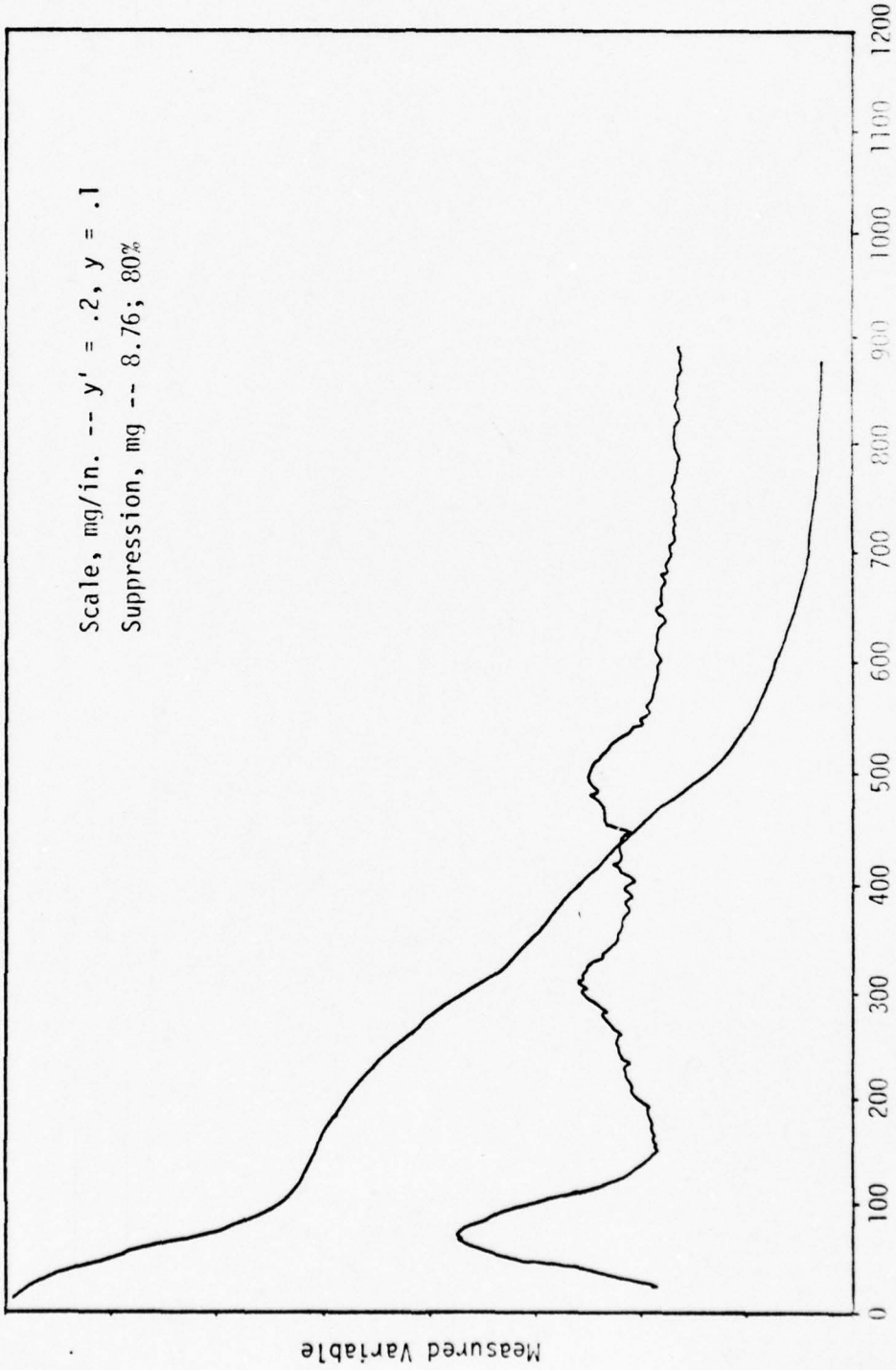

Figure 4.4. TGA Pattern, Sample B5, H2

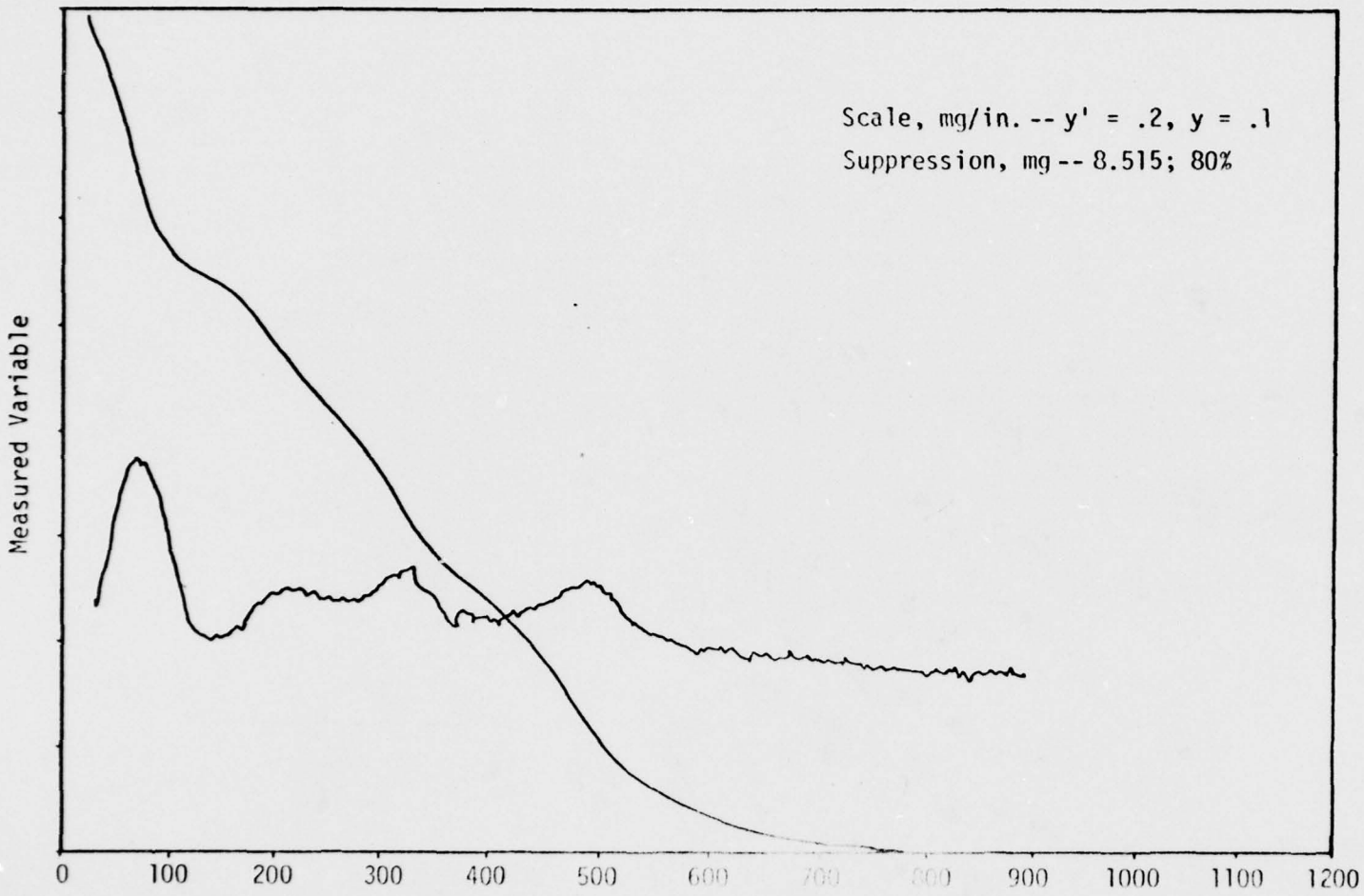

Figure 4.5. TGA Pattern, Sample 06, M4.

of minerals. The endothermic reactions indicated by thermograms in Figures 4.3-4.5 indicate the presence of both gibbsite and kaolinite. The quantities calculated for this particular soil are approximately 22 percent kaolinite and 6 percent gibbsite.

Knowledge of the quantity of kaolinite and the intensity of the kaolinite peak allows an estimation of the quantities of the remaining soil components to be made. This is strictly a relative measurement but an estimation of the clay fraction in terms of percentage composition can be made.

Montmorillonite	65 - 70%
Illite and Trace Minerals	3 - 5%
Kaolinite	20 - 25%
Gibbsite and Allophane	5 - 7%

The primary constituent of the non-clay materials in the soil sample is quartz.

The dominance of montmorillonite in this soil sample supports further the indication of the phase relationships of this soil. Montmorillonite characteristically has high liquid and plastic limits and the associated swelling and shrinking properties. Both compressibility and hydraulic conductivity are strong functions of soil composition. In this case the compressibility of montmorillonite is quite high and the hydraulic conductivity is low, which again will create construction problems and affect the rate of pore pressure dissipation.

Stress-Strain Behavior

The stress-strain relationships of both the undisturbed and representative remolded specimens are illustrated in Figures 4.6 through 4.16. These graphs show the deviator stress vs. axial strain relationship. Included also are the $\bar{\sigma}_1/\bar{\sigma}_3$ relationship and the pore pressure response related to increased stresses and undrained conditions.

The deviator stress vs. axial strain curves for the undisturbed tests show relatively distinct peaks before a constant residual strength is achieved. The peak values are obtained at low strain while the residual strength is a long term resultant. The distinct peaking of the undisturbed sample curves indicate a strongly developed mineral framework. The resultant fabric is rigid and the stability of the system enhanced. The fact that extremely high void ratios exist for this soil also indicates the flocculated nature of the particles. Apparently the soil particles form an open, skeleton type structure which is bonded and relatively stable. As the applied load and resultant internal strains increase, the soil fabric begins to collapse and bonds break. Once the structure can no longer resist these local failures the specimen ruptures and ultimate failure occurs. The breaking of the bonds and the reorientation of the soil particles result in lower long-term strength. All specimens failed along distinct failure planes extending through the various laminations with no apparent resistance by the sand/silt layers.

Throughout the loading sequence pore pressure increased at a constant rate coincident with the increase in stresses. As the structure collapsed more and more of the load was transferred to the pore

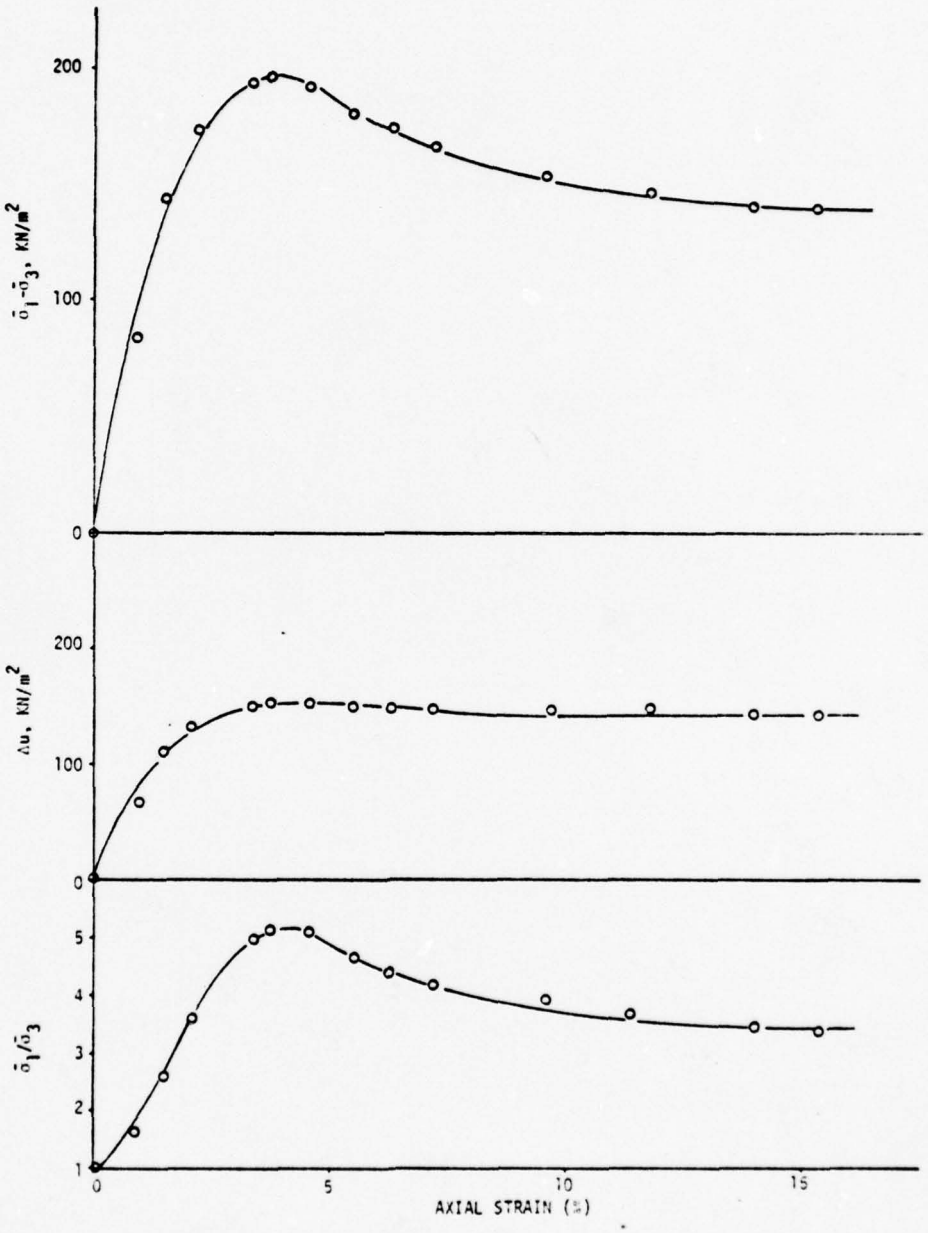

Figure 4.6. Sample B3, M9, Undisturbed, σ_c = 200 KN/m^2

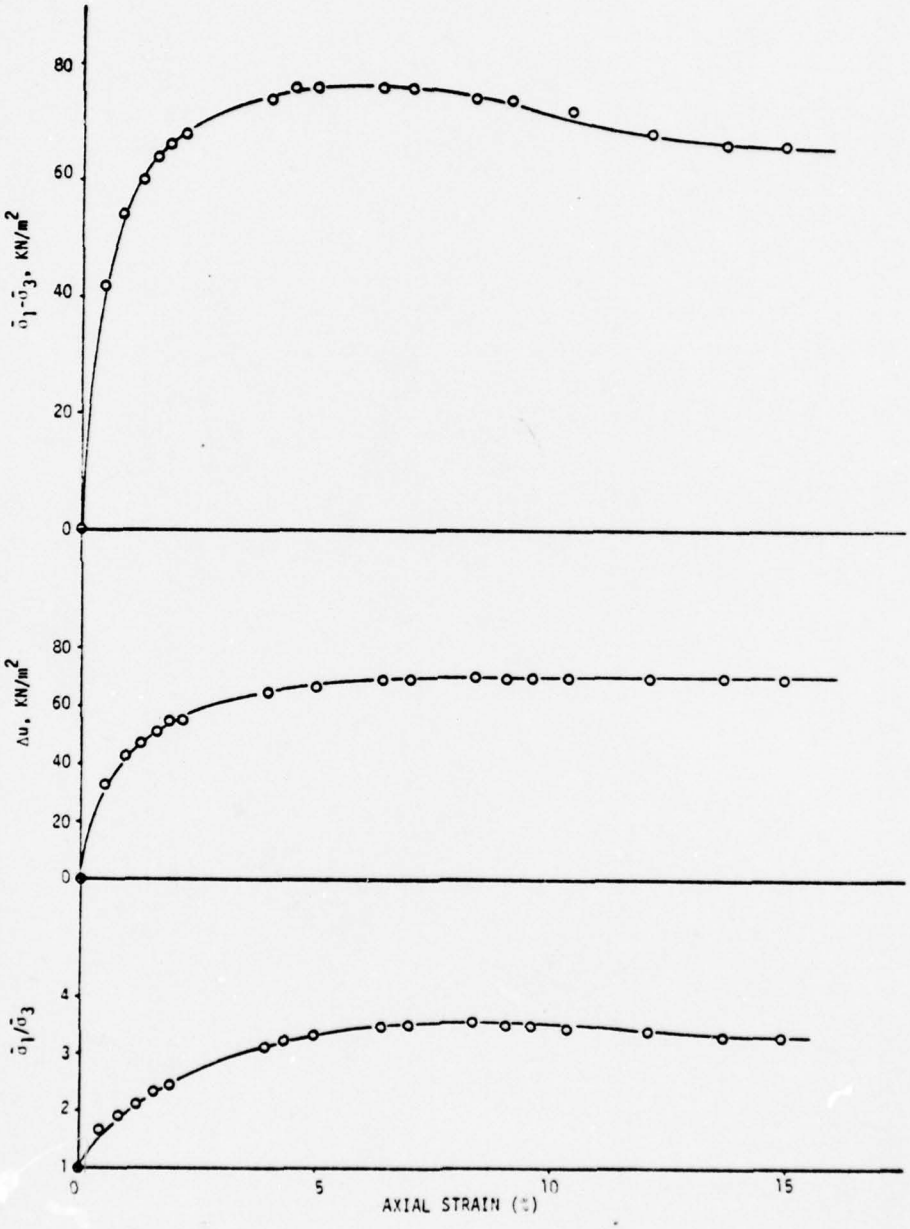

Figure 4.7. Sample B5, M2, Undisturbed, σ_c = 100 KN/m^2

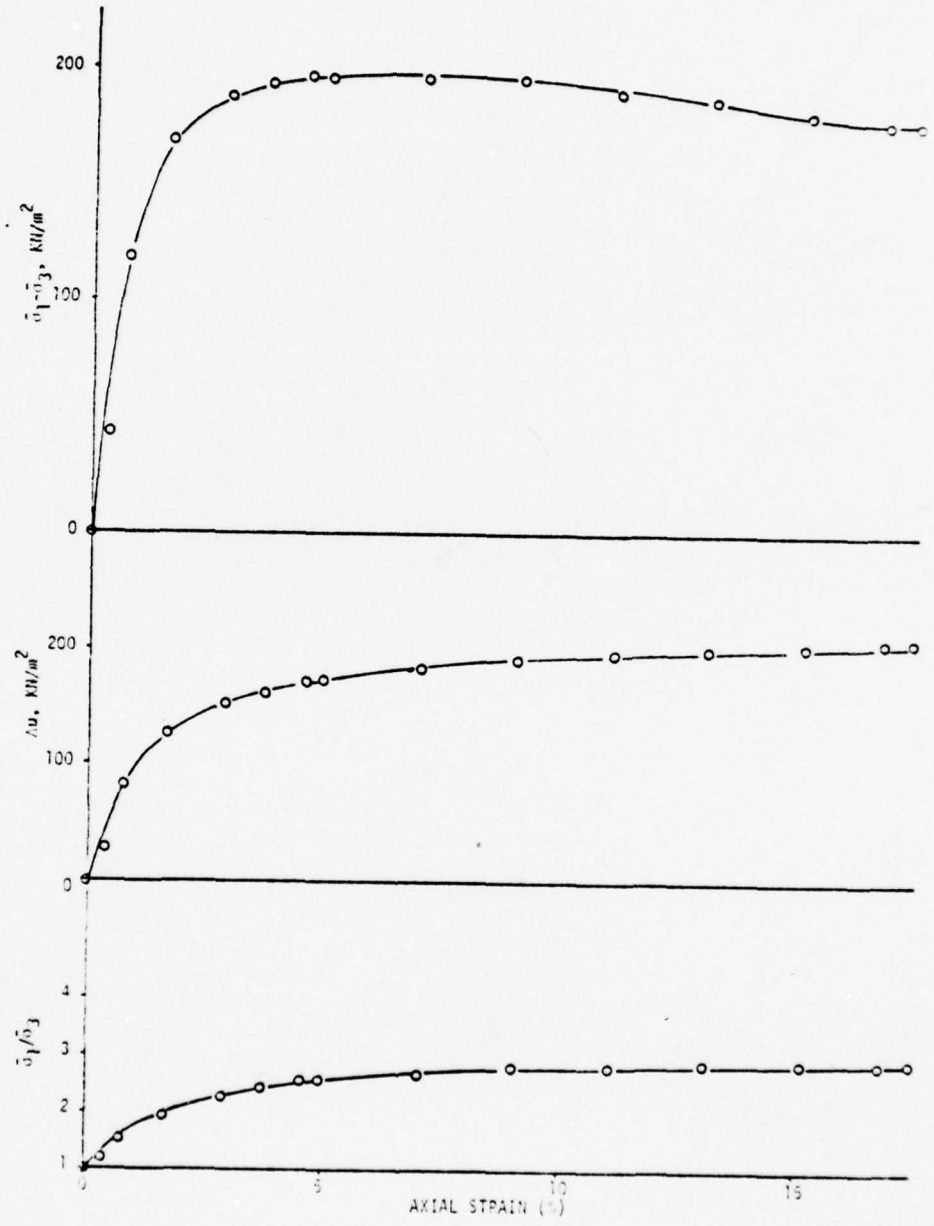

Figure 4.8. Sample B5, M2, Undisturbed, σ_c = 300 KN/m^2

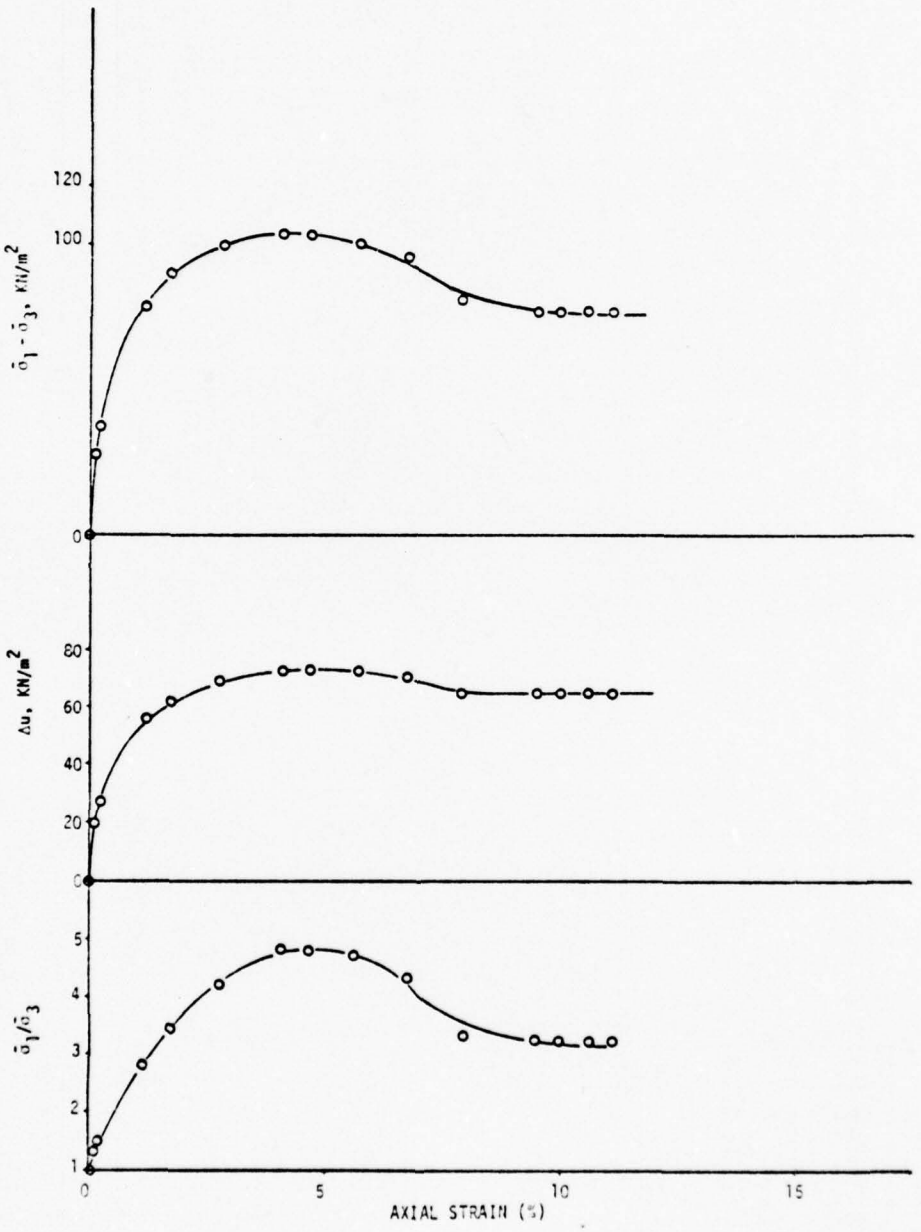

Figure 4.9. Sample B6, M4, Undisturbed, σ_c = 100 KN/m^2

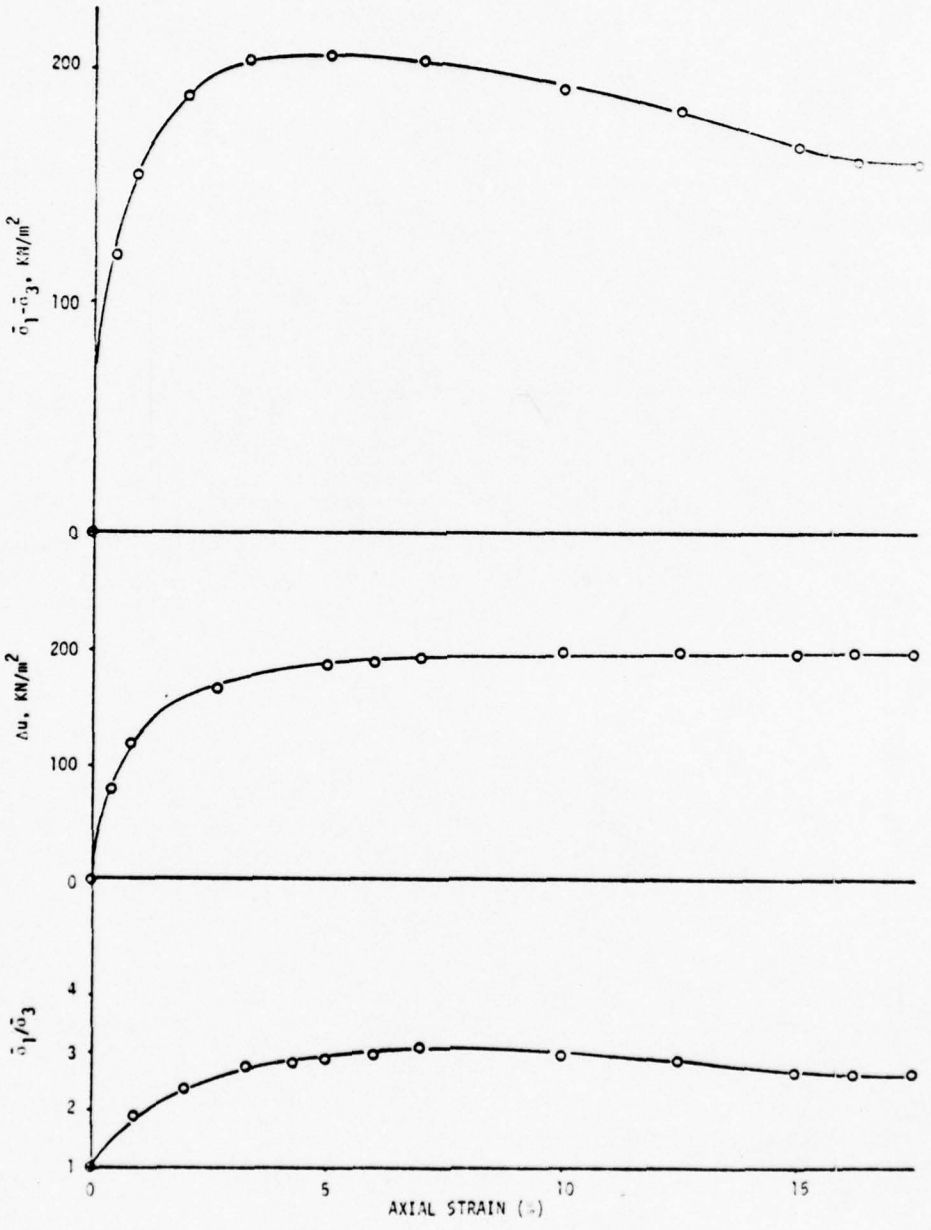

Figure 4.10. Sample B6, M4, Undisturbed, σ_c = 300 KN/m^2

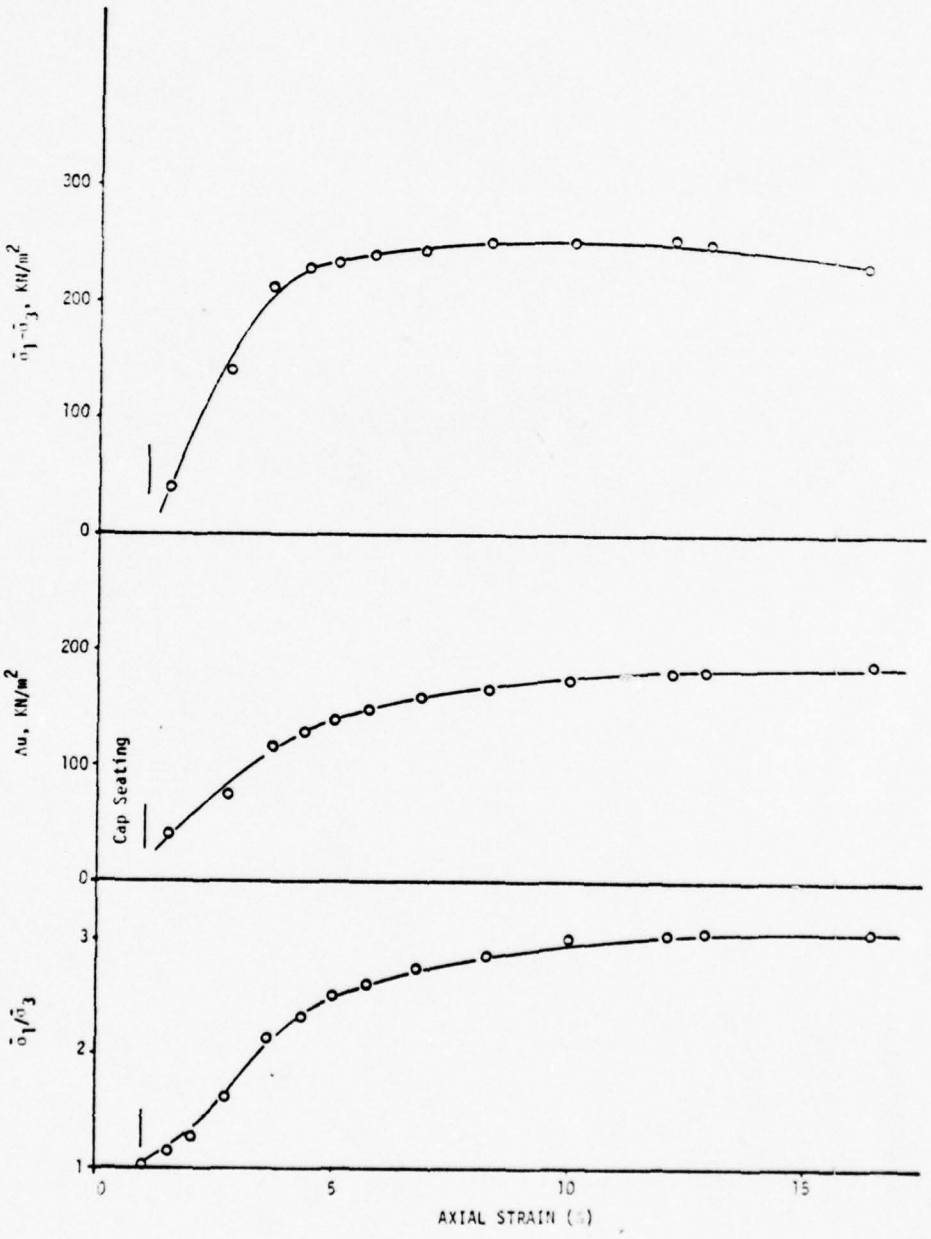

Figure 4.11. Sample C3, M4, Undisturbed, σ_c = 300 KN/m^2

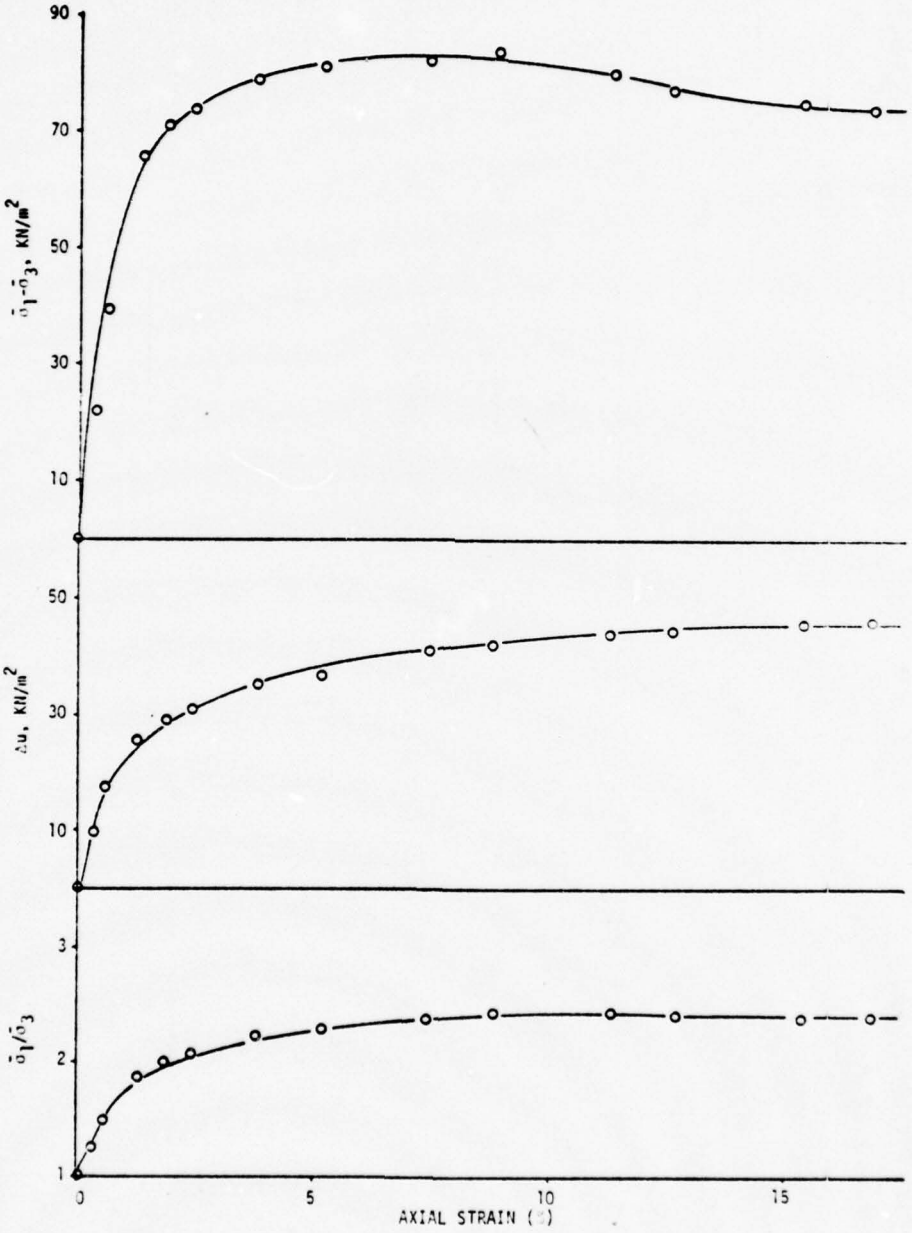

Figure 4.12. Sample C3, M4, Undisturbed, σ_c = 100 KN/m^2

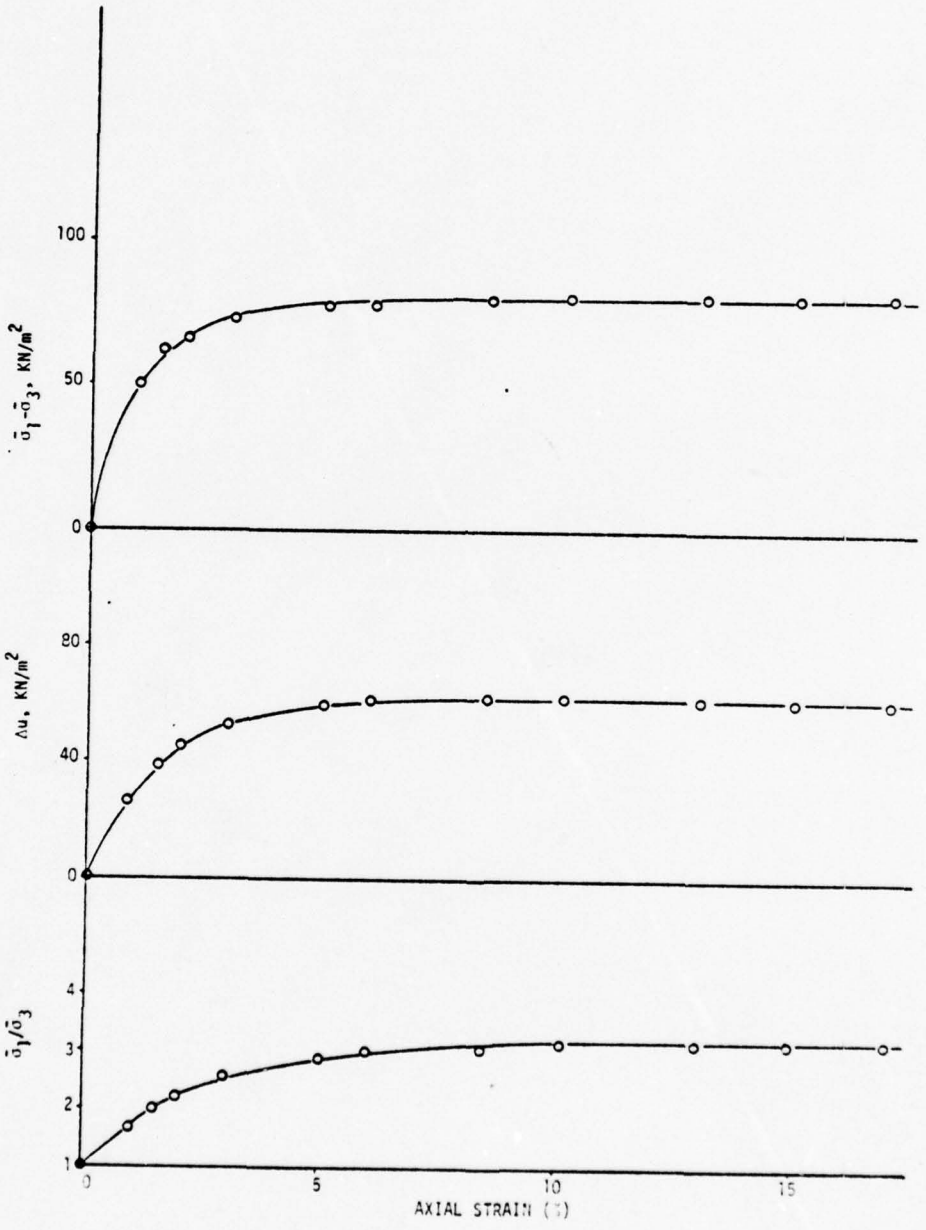

Figure 4.13. Sample B5, M2, Remolded, σ_c = 100 KN/m^2

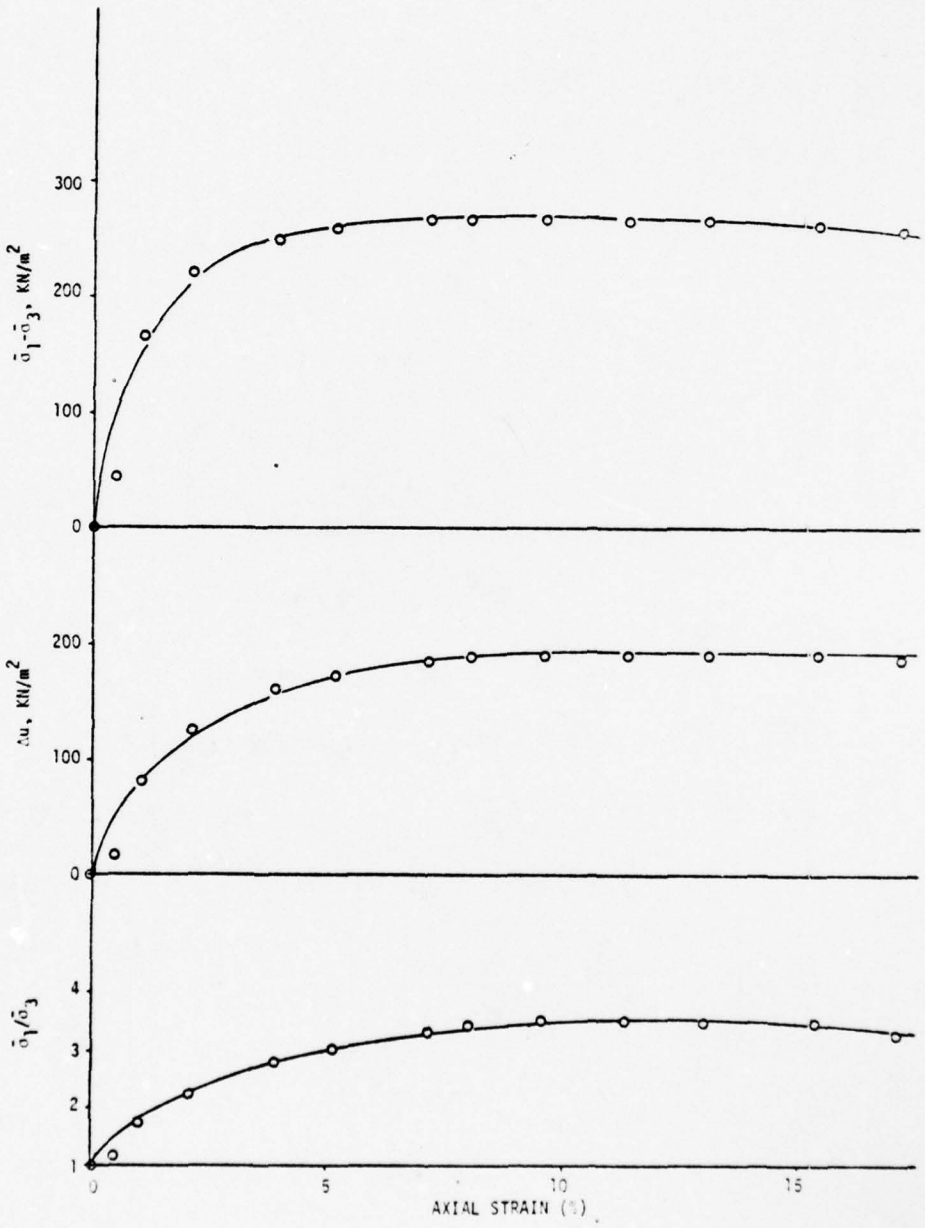

Figure 4.14. Sample B5, M2, Remolded, σ_c = 300 KN/m^2

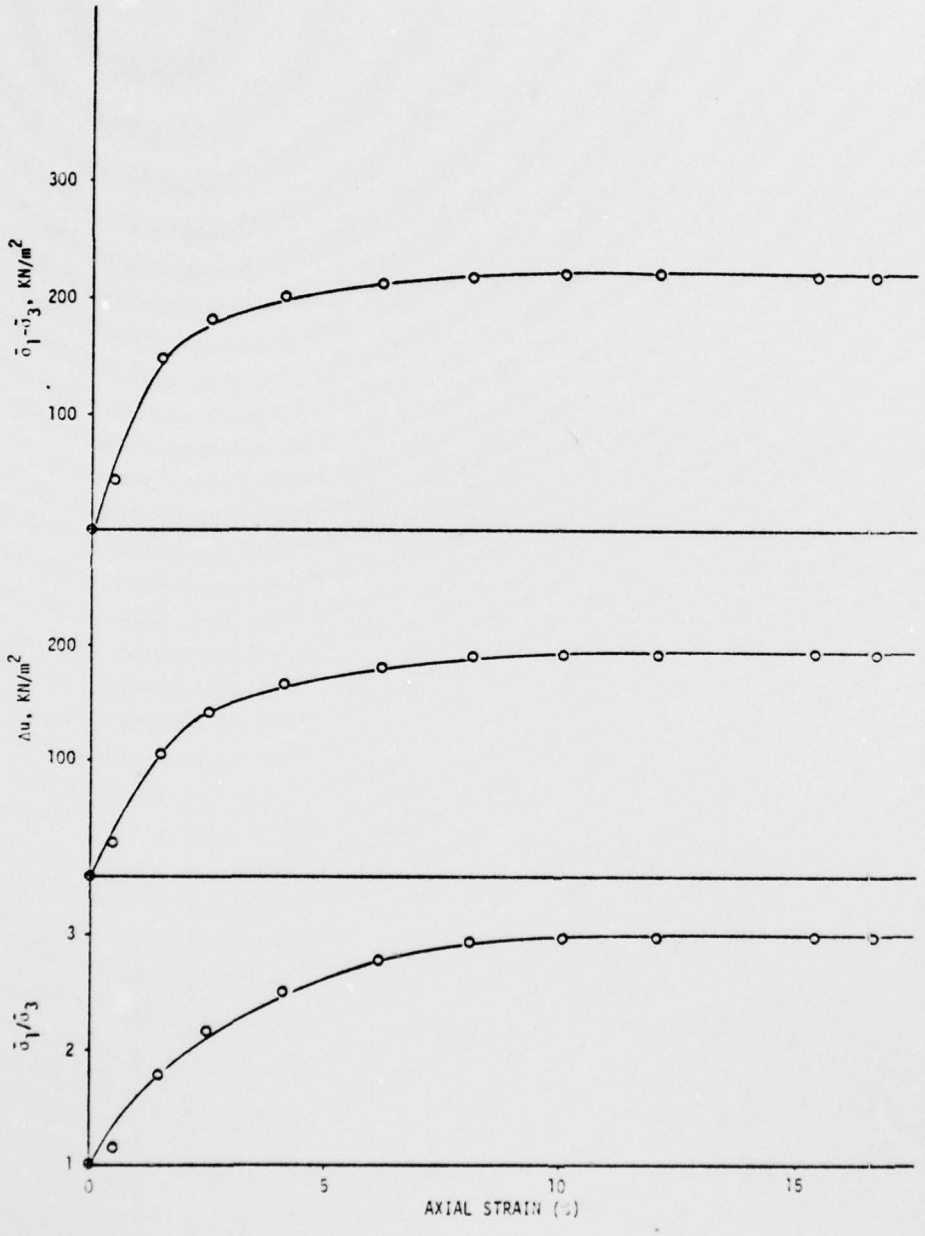

Figure 4.15. Sample C3, M4, Remolded, σ_c = 100 KN/m^2

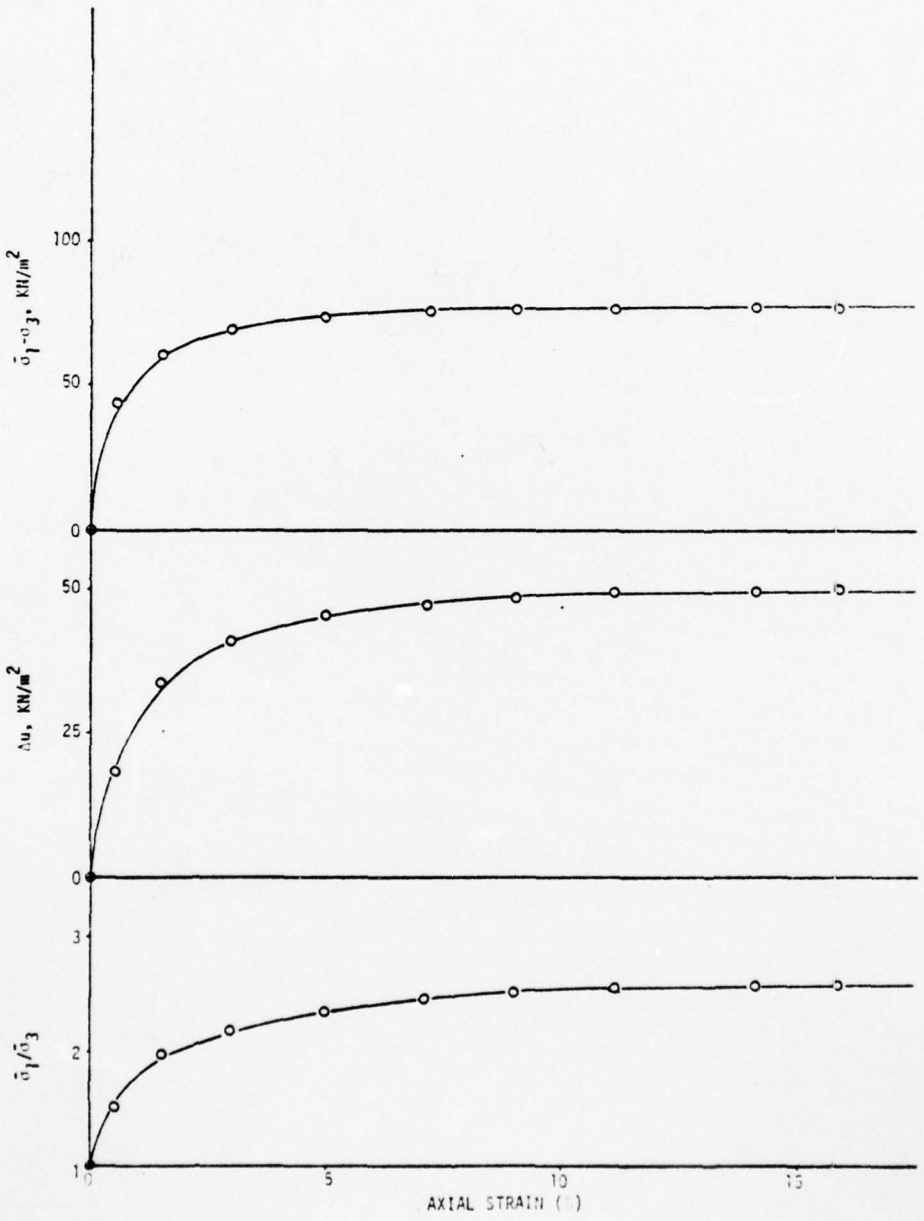

Figure 4.16. Sample C3, M4, Remolded, σ_c = 300 KN/m^2

fluid. Once failure occurred, the load and pore pressures remained constant.

The remolded samples do not display the dintinct peaks at maximum deviator stress. The soil reaches an ultimate shear strength and remains there as it deforms continually and remains in a plastic state. This condition is characteristic of an unbonded, random fabric. Because of the weakness of the remolded samples there will be a flatter slope to the stress-strain curves. The remolded samples were homogeneous in nature and no longer resembled the undisturbed soil makeup.

Comparison of Undisturbed and Remolded Strengths

Some of the deviator stress values for the remolded specimens appear to be higher than those measured for the undisturbed samples. The reason for this apparent inconsistency is the fact that the remolded samples were tested at much lower moisture contents. Therefore, higher strengths were measured. The soil remolded at the natural moisture content had no structural integrity and existed in liquid form, and could not be evaluated with available equipment. This result is an indication of the apparent sensitive nature of this soil.

Since there is a definite relationship between moisture content at failure and shear strength for normally consolidated cohesive soils (14), the soil was mixed at moisture contents near 70 percent which allow a specimen to be tested in the conventional triaxial apparatus. Plotting the results of these tests allows the prediction of strength values for high moisture contents (Figure 4.17). Note the significant reduction in strength and shifting of the linear relationships once the

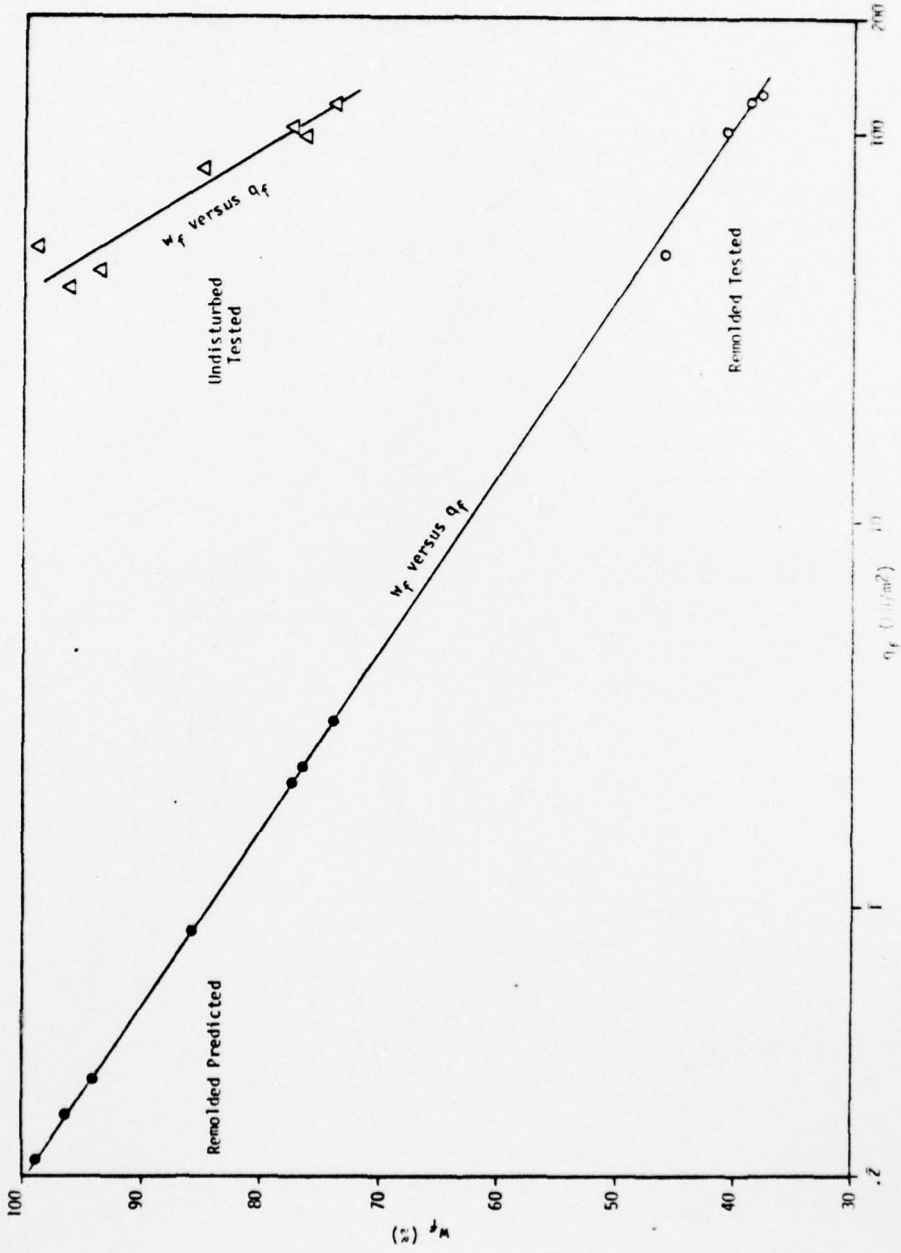

Figure 4.17. w_f versus q_f Relationships

soil is remolded at the undisturbed failure moisture contents. The scatter observed in this data may be attributed to the quantity and effect of varves and the initial moisture contents of each specimen. With this relationship a comparison of undisturbed and remolded strengths may be made and the degree of sensitivity evaluated (Table 4.2). A definite sensitivity to remolding is observed for all soil samples.

Table 4.2. Shear Strength Comparison

Sample	Consolidation Pressure σ_c (kN/m^2)	Final Water Content %	q_f (Undisturbed) kN/m^2	q_f (Remolded) kN/m^2	Sensitivity
B3, M9	200	85.8	96	3.3	29
B5, M2	100	96.4	38	1.1	35
	300	76.7	96	9	11
B6, M4	100	99.0	52	.25	208
	300	77.5	106	8	13
C3, M4	100	94.0	42	1.4	30
	300	74.0	118	11.5	10

Shear Strength Parameters

The relationships between the total stress, pore pressure and effective stress characteristics obtained from the consolidated-undrained triaxial tests on the undisturbed specimen are illustrated in Figures 4.18 through 4.20. The stress paths obtained from the remolding of a composite sample of the soil is shown in Figure 4.21. A mixing of the soils was required to provide sufficient quantities of material, at the same initial moisture content, to insure representative triaxial test

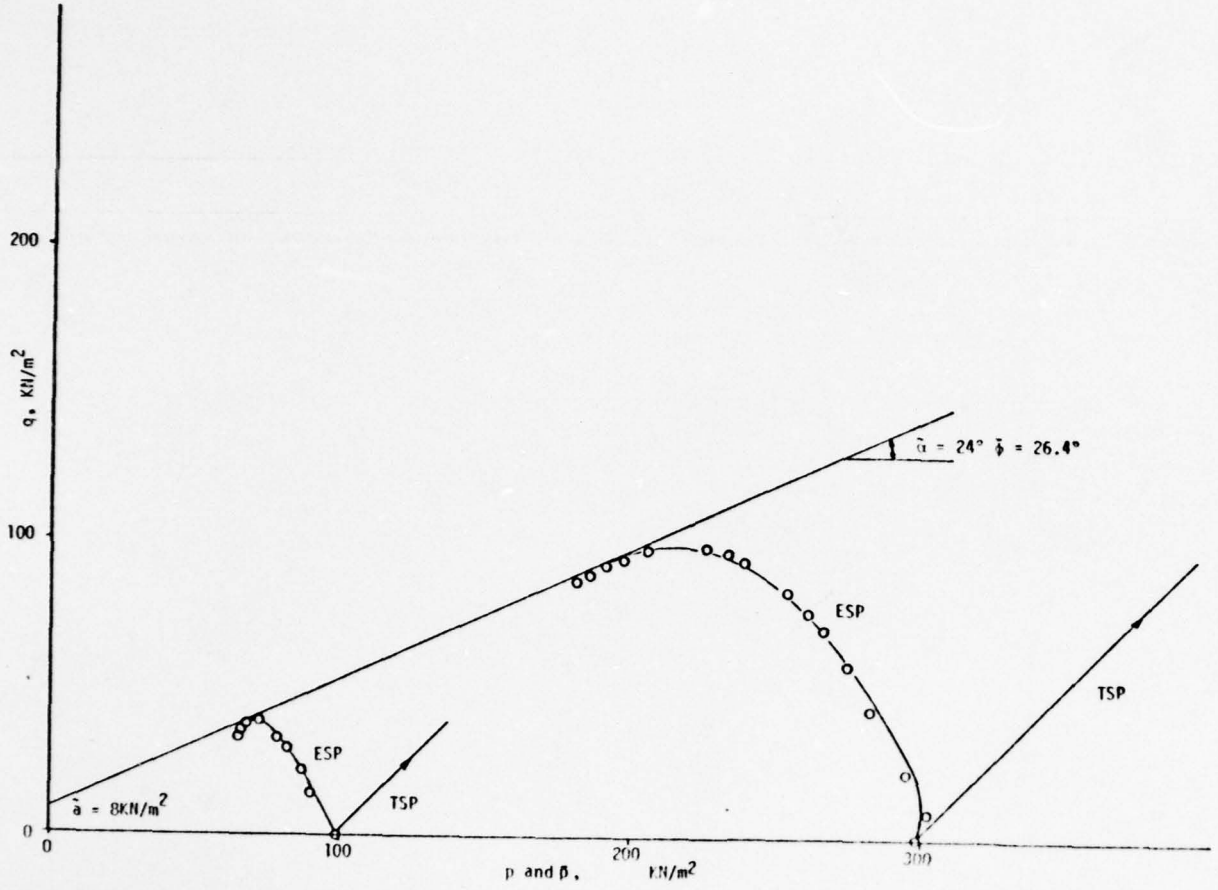

Figure 4.18. Stress Paths and Data for CU Triaxial Test on Undisturbed Sample B5, M2

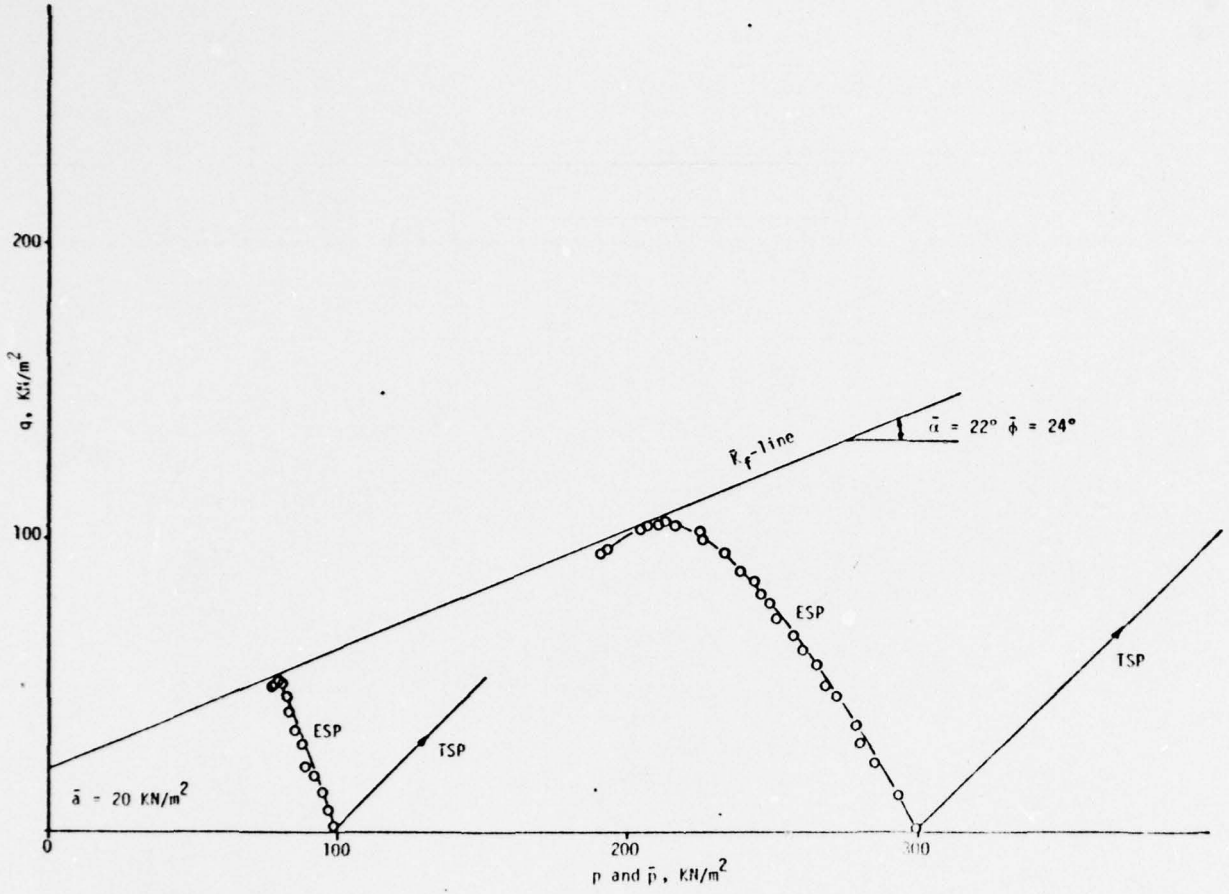

Figure 4.19. Stress Paths and Data for CU Triaxial Test on Undisturbed Sample B6, M4

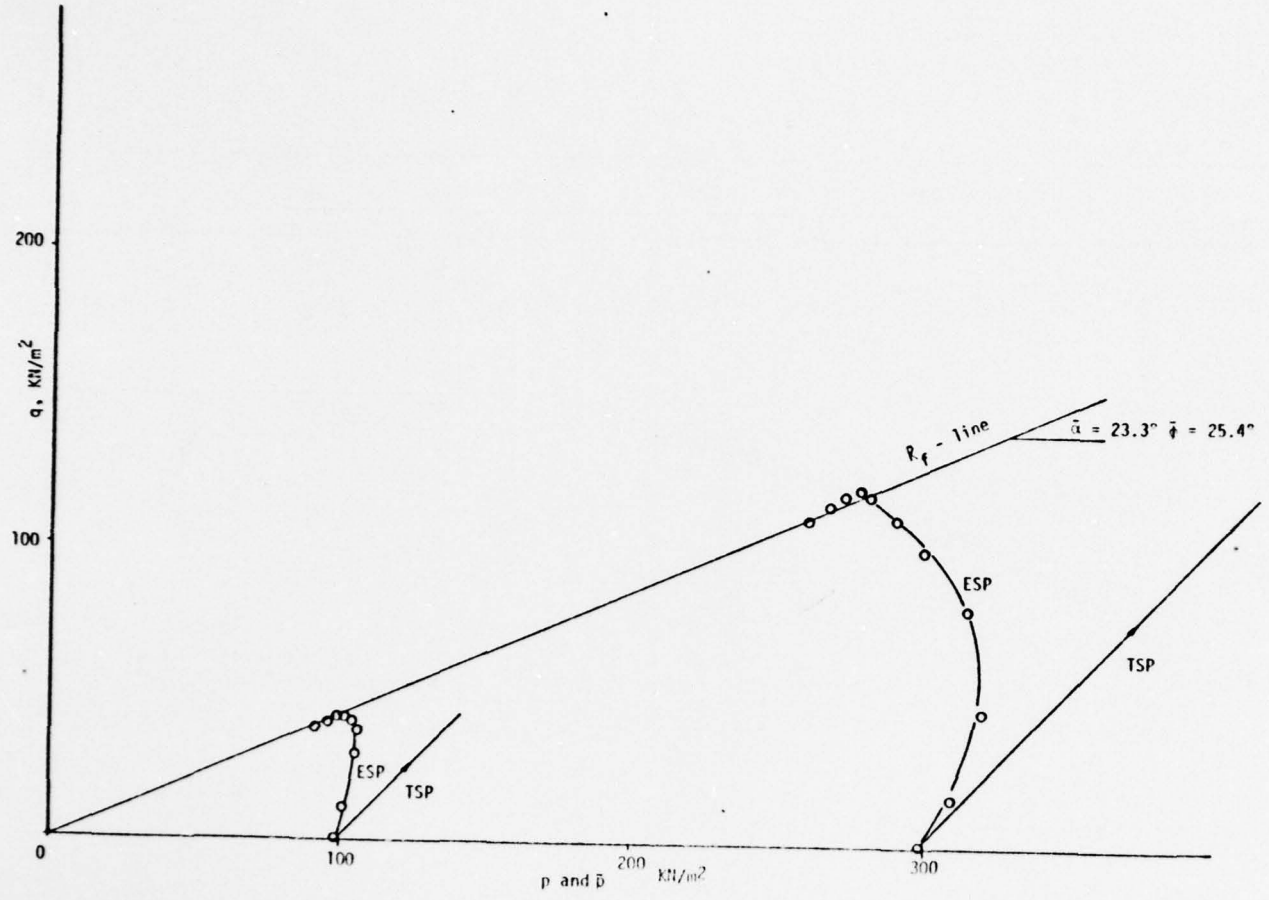

Figure 4.20. Stress Paths and Data for CU Triaxial Test on Undisturbed Sample C3, M4

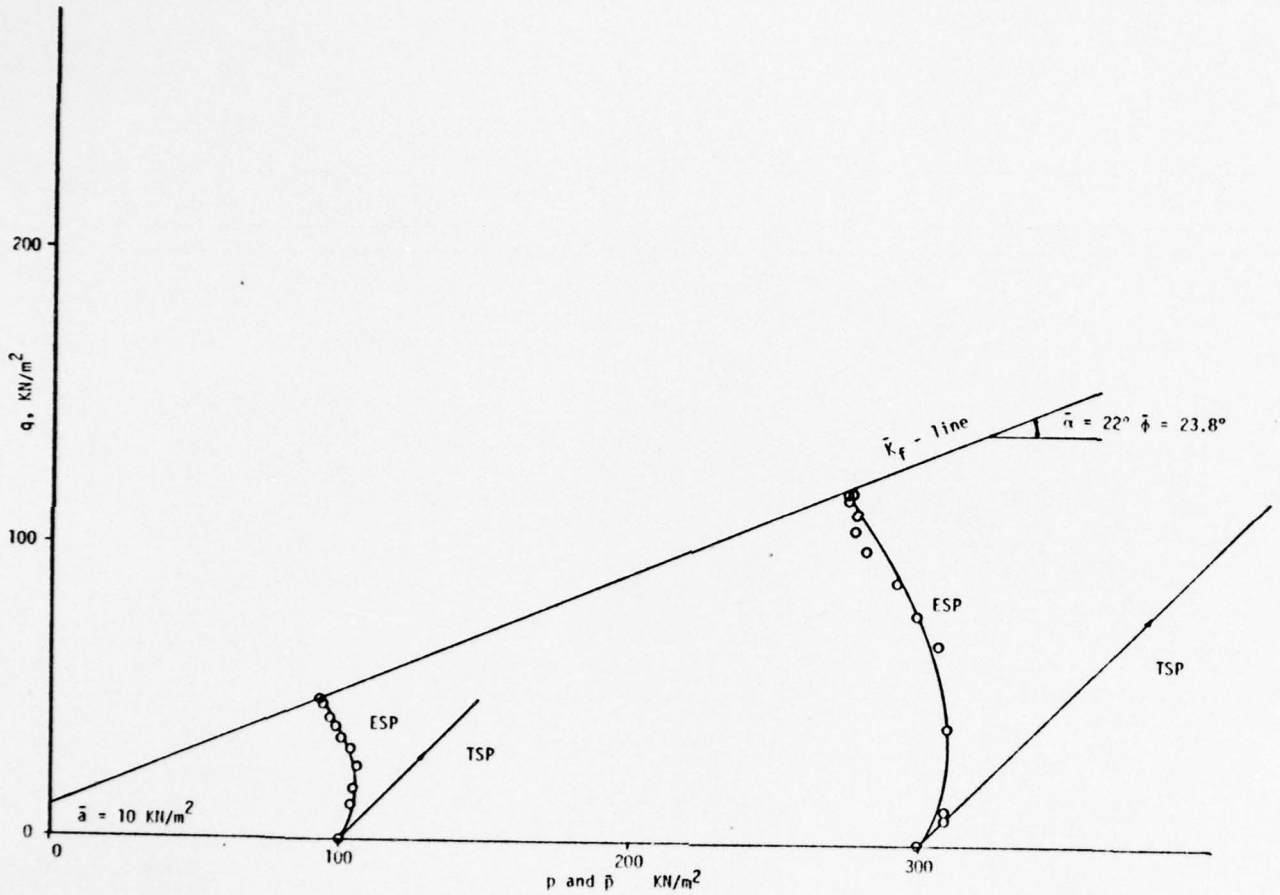

Figure 4.21. Stress and Data for CU Triaxial Test on Composite Remolded Sample

results. The effective stress paths show definite leftward curvature, characteristic of a normally consolidated cohesive soil. No difficulty existed concerning the definition of failure. Once the failure condition was reached, the stress states dropped off or followed the failure envelope. All figures showed a consistency of measured values to include the remolded specimens.

The parameters obtained from these diagrams are vital in conducting a stability analysis and design, as well as in predicting possible pore pressure changes during and after the construction sequence. Table 4.3 lists parameters measured for the undisturbed soil samples. The pore pressure parameter, A_f, falls into the normally consolidated range of 0.7 to 1.3 as given by Bjerrum (14). Higher values for A_f (1.5 - 2.5) (14) would be suspected due to other indications of the possible sensitive nature of this material.

Table 4.3. Shear Strength Parameters

Sample	$\bar{a}$(kN/m^2)	$\bar{\alpha}$(°)	$\bar{c}$(kN/m^2)	$\bar{\phi}$(°)	A_f σ_c=100kN/m^2	A_f σ_c=300kN/m^2
Undisturbed						
B5, M2	8	24	9	26.4	.96	1.03
B6, M4	20	22	22	24.0	.68	.96
C3, M4	0	23.3	0	25.4	.59	.57
Remolded						
Composite	10	22	11	23.8	.56	.62

Varved System Observations

All undisturbed samples contained distinct varves within the tested specimens. Sample B3, M9 contained the greatest number of laminations while sample C3, M4 had the least. This is reflected by the relatively high clay content of the latter sample. Investigation of the soil showed that the coarse grain layers were relatively dry and that the high moisture levels were retained in the clay material. Depending upon the length of the coarse grain layers, they would provide excellent drainage faces and assist in pore pressure dissipation and consolidation.

The failure planes for the undisturbed samples passed directly through the horizontal varves without distortion. The clays exhibited a flocculated type structure which is typical of the soft varved clays of eastern Canada (21). Remolding the samples resulted in a homogeneous mixture of all particle sizes. The failure associated with these specimens was a bulge type due to a plastic flow of the material. The strength characteristics have been indicated previously.

V. CONCLUSIONS AND RECOMMENDATIONS

Conclusions drawn from this study, and recommendations for further research are presented in this chapter. The findings and recommendations resulting from this study are based on laboratory test results and are limited to the specific varved soil tested. Application of these test results to other areas would not be advisable due to the inherent variability of soil conditions at new locations.

Conclusions

A series of consolidated-undrained triaxial compression tests were performed on undisturbed and remolded samples of normally consolidated varved clay. The tests were used to determine the shear strength characteristics of both undisturbed and remolded specimens. The following conclusions can be made for this type soil and the testing procedure employed:

1. The soil has a definite sensitive nature with a relatively high loss of strength when remolded at the same moisture content.

2. The liquidity index and A_f parameters do not appear to be accurate indications of sensitivity for this varved system. This may be attributed to the non-homogenity and anisotropic characteristics of the soil. The inherent mixing of layers in determining physical soil properties does not provide reliable phase relationships.

3. A marked soil fabric difference between the undisturbed varved system and the remolded specimens exist. The undisturbed samples had a flocculated clay assemblage and were stable at high moisture contents. The remolded specimens displayed a dispersed nature and were stable only at low moisture contents. This characteristic is typical of the varved clay studied in the northern hemisphere.

4. The undisturbed and remolded specimens have different failure characteristics. The undisturbed samples showed a somewhat brittle nature and failed along a distinct shear plane, suggesting the formation of particle bonds during deposition. Remolded specimens bulged at failure and maintained a constant shear strength after failure.

5. The shear strength parameters measured for both the undisturbed and composite remolded specimens were relatively consistent. The $\overline{\phi}$ value decreased slightly with remolding.

6. Mineralogically, the clay fraction of the soil is primarily smectitic in nature and displays the characteristically high moisture contents, Atterberg limits, and shrink-swell properties.

7. The test procedures and equipment utilized provide reliable parameters for design and analysis of structures associated with this particular site.

Recommendations

It is recommended that research studies be undertaken to extend the knowledge developed from this study. An investigation similar to this study but for different areas of the southern hemisphere would determine the validity of the conclusions and whether the measured characteristics would apply to a variety of site locations. A more in-depth

study of the exact mineralogical composition would provide a basis for studies in numerous areas of geotechnical engineering. Studies as to why liquidity index and pore pressure parameter A_f are not indicative of the sensitivity of a varved system would be beneficial. Research pertaining to the consolidation characteristics of the soil used in this study would also provide valuable engineering knowledge.

AD-A051 618 AUBURN UNIV ALA F/G 8/7
A STUDY OF THE SHEAR STRENGTH OF NORMALLY CONSOLIDATED ECUADORI--ETC(U)
DEC 77 J A BALL

UNCLASSIFIED NL

2 OF 2
AD
A051618

END
DATE
FILMED
4-78
DDC

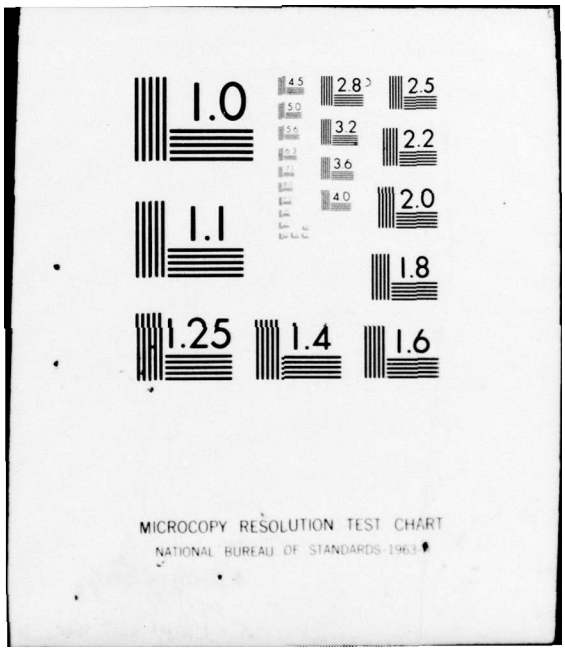
1.0
1.1
1.25
1.4
1.6
1.8
2.0
2.2
2.5
2.8
3.2
3.6
4.0
4.5
5.0
MICROCOPY RESOLUTION TEST CHART
NATIONAL BUREAU OF STANDARDS-1963

REFERENCES

1. Bishop, A. W., "The Strength of Soils as Engineering Materials," Geotechnique, Vol. 16, No. 2, 1966, pp. 91-94.

2. Bishop, A. W. and Bjerrum, L., "The Relevance of the Triaxial Test to the Solution of Stability Problems," Proc. ASCE Research Conf. o Shear Strength of Cohesive Soils, Boulder, Col., 1960, pp. 437-501.

3. Bishop, A. W. and Henkel, D. J., The Measurement of Soil Properties in the Triaxial Test, Edward Arnold Ltd., London, 1964.

4. Bjerrum, L. and Wu, T. H., "Fundamental Shear Strength Properties of the Lilla Edet Clay," Geotechnique, Vol. X, No. 3, 1960, pp. 101-109.

5. Brown, G., The X-Ray Identification and Crystal Structures of Clay Minerals, Jarrold and Sons Ltd., Norwich, 1961.

6. Crawford, C. B., "Cohesion in an Undisturbed Sensitive Clay," Geotechnique, Vol. XIII, No. 2, 1963, pp. 132-145.

7. Donaghe, R. T. and Townsend, F. C., Effects of Anisotropic Versus Isotropic Consolidation in Consolidated-Undrained Triaxial Compression Tests of Cohesive Soils, TR S-75-13, Waterways Experiment Station, 1973.

8. Espenshade, E. B., ed., Goode's World Atlas, Chicago, Rand McNally and Co., 1964.

9. Houston, W. N. and Mitchell, J. K., "Property Interrelationships in Sensitive Clays," J. Soil Mech. Found. Div., ASCE, Vol. 95, No. SM4, Proc. Paper 6666, July, 1969, pp. 1037-1062.

10. Hvorslev, M. J., Subsurface Exploration and Sampling of Soil for Civil Engineering Purposes, Engineering Foundation, ASCE, 1965.

11. Hvorslev, M. J., Physical Properties of Remolded Cohesive Soils, Translation No. 69-5, Waterways Experiment Station, 1969.

12. Kenney, T. C., "Pore Pressures and Bearing Capacity of Layered Clays," J. Soil. Mech. Found. Div., ASCE, Vol. 90, No. SM4, 1964, pp. 27-55.

13. Ladd, C. C., "Stress-Strain Behaviour of Anisotropically Consolidated Clays During Undrained Shear," Proc. 6th Inter. Conf. Soil Mech. Found. Eng., Vol. 1, 1963, pp. 282-286.

14. Lambe, T. W. and Whitman, R. V., Soil Mechanics, John Wiley and Sons, Inc., New York, 1969.

15. Lee, K. L. and Shubeck, R. J., "Plane-Strain Undrained Strength of Compacted Clay," J. Soil. Mech. Found. Div., ASCE, Vol. 97, No. SM1, 1971, pp. 219-233.

16. Lo, K. Y. and Milligan, V., "Shear Strength Properties of Two Stratified Clays," J. Soil. Mech. Found. Div., ASCE, Vol. 93, No. SM1, Proc. Papers 5056, January, 1967, pp. 1-15.

17. Milligan, V., Soderman, L. G. and Rutka, A., "Experience with Canadian Varved Clays," J. Soil. Mech. Found. Div., ASCE. No. SM4, 1962, pp. 31-67.

18. Mitchell, J. K., Fundamentals of Soil Behavior, John Wiley and Sons, Inc., New York, 1976.

19. Mitchell, J. K. and Houston, W. N., "Causes of Clay Sensitivity," J. Soil. Mech. Found. Div., ASCE, Vol. 95, No. SM3, Proc. Paper 6568, May, 1969, pp. 845-871.

20. Parsons, J. D., "New York's Glacial Lake Formation of Varved Silt and Clay," J. Geotechnical Engr. Div., ASCE, Vol. 102, No. GT6, 1976, pp. 605-638.

21. Quigley, R. M. and Ogunbadejo, T. A., "Clay Layer Fabric and Oedometer Consolidation of a Soft Varved Clay," Canadian Geotechnical Journal, Vol. 9, 1972, pp. 165-175.

22. Rowe, P. W., "Consolidation of Lacustrine Clay," Geotechnique, Vol. 9, 1959.

23. Shield, R. T., "On Coulomb's Law of Failure in Soils," J. Mechanics and Physics of Solids, Vol. 4, 1955, pp. 10-16.

24. Skempton, A. W., "The Pore Pressure Coefficient A and B," Geotechnique, Vol. 4, 1954, pp. 143-147.

25. Sowers, G. B. and Sowers, B. F., Introductory Soil Mechanics and Foundations, Macmillan, New York, 1970.

26. Spence, R. A. and Glynn, T. E., "Shear Characteristics of a Marine Clay," J. Soil. Mech. Found. Div., ASCE, Vol. 88, No. SM4, 1962, pp. 86-107.

27. Stokes, W. L., Essentials of Earth History, 3rd Edition, Prentice Hall, Inc., Englewood Cliffs, 1973.

28. Terzaghi, K. and Peck, R. B., Soil Mechanics in Engineering Practice, John Wiley and Sons, Inc., New York, 1967.

29. Townsend, D. L., Hughes, G. T. and Cruickshank, J. A., "The Effect of Pore Pressures on the Undrained Strength of a Varved Clay," Proc. 6th Inter. Conf. Soil Mech. Found. Eng., Vol. 2, pp. 385-389.

30. Tschebotarioff, G. P. and Bajliss, J. R., "The Determination of the Shearing Strength of Varved Clays and Their Sensitivity of Remolding," Proc., 2nd Inter. Conf. Soil Mech. Found. Eng., Vol. 1, 1948, pp. 203-207.

31. Vaid, Y. P. and Campanella, R. G., "Triaxial and Plane Strain Behavior of Natural Clay," J. Geotechnical Engr. Div., ASCE, Vol. 100, No. GT3, 1974, pp. 207-224.

32. Walker, F. C. and Irwin, W. H., "Engineering Problems in Columbia Basin Varved Clay," J. Soil Mech. Found. Div., ASCE, Vol. 80, 1954, Proc. Papers 515.

33. Yong, R. N. and McKyes, E., "Yield and Failure of a Clay Under Triaxial Stresses," J. Soil. Mech. Found. Div., ASCE, Vol. 97, No. SM1, 1971, pp. 159-176.

34. Personal correspondence to Dr. R. K. Moore from Dr. J. E. Laier, Letter of Transmittal, Guayaquil Soil Data.

35. Personal correspondence to Dr. R. K. Moore from Dr. F. C. Townsend, Suggested Modifications to Triaxial test procedure.

36. Class Notes, AY 656, "Clay Mineralogy," Auburn University, 1976, Benjamin F. Hajek, Ph.D.

APPENDIX